UNIVERSITY OF GHANA

EVALUATING THE PERFORMANCE OF CMRI FOR ESTIMATING THE SPATIAL DISTRIBUTION OF MANGROVES AT THE KETA LAGOON COMPLEX IN THE VOLTA REGION OF GHANA

SACKEY-ADDO SAMUEL

(10487371)

A DISSERTATION SUBMITTED TO THE DEPARTMENT OF MARINE AND FISHERIES SCIENCES IN PARTIAL FULFILLMENT OF THE REQUIREMENTS FOR THE AWARD OF A MSc. (Hons) DEGREE IN

COASTAL ZONE MANAGEMENT

OCTOBER, 2020

DECLARATION

This dissertation is the result of research work undertaken by Samuel Sackey-Addo in the Department of Marine & Fisheries Sciences, University of Ghana, Legon, under the supervision of Professor George Wiafe and Dr. Kwame Adu Agyekum of the Department of Marine and Fisheries Sciences.

SACKEY-ADDO SAMUEL
(STUDENT)

SIGNATURE: .....

03-OCTOBER-2020
DATE: .....

PROFESSOR GEORGE WIAFE
(SUPERVISOR)

SIGNATURE: ……..

28-OCTOBER-2020
DATE: .....

DR. KWAME ADU AGYEKUM
(SUPERVISOR)

SIGNATURE: .....

28-OCTOBER-2020
DATE: .....

ABSTRACT

Data obtained from remote sensing is useful for evaluating and mapping infrastructure and natural resources including vegetation. Over the past years, a number of vegetation indices have been developed to detect vegetation with the use of satellite imageries to monitor the distribution and phenology of mangroves. Forest managers and environmental scientists have developed a wide range of indices for delineating and assessing the health of different vegetation and forest cover. This study will evaluate the performance of Combined Mangrove Recognition Index (CMRI) for estimating and distinguishing mangroves in the Keta Lagoon Complex. The CMRI was compared to the Normalized Vegetation Index (NDVI), a widely used vegetation index and supervised classification (maximum likelihood) which were selected based on their classification accuracies of about 80% in the estimation of vegetation. Sentinel-2 imagery was used to generate vegetation maps for the NDVI and CMRI indices and a land cover map generated using the supervised classification (maximum likelihood) technique. The threshold value method was used to extract the values of mangrove areas for each index and used to delineate areas of mangrove and non-mangrove using binary data with the use of UAV imagery for validation. Random points with their coordinates were generated as reference points on the UAV imagery and overlaid on the other maps. Areas of mangroves were denoted "1" and areas with non-mangroves were denoted "0". The Cochran's Q test, used for statistical analysis of binary data was used to derive the p-value after which the area coverage of mangroves in the study area was estimated. From the study, the threshold values used to mask out mangroves were observed to be between 0.27 and 0.37, and between 0.51 and 0.70 for NDVI and CMRI respectively. UAV imagery was used to validate the area coverage due to its high resolution. The imagery covered an area of 1.8 km^2 and was used as a subset for the mangrove area coverage comparison. Mangrove area coverage was estimated to be 0.32km^2,

0.30km^2, and 0.25km^2 for NDVI, supervised classification and CMRI respectively. All techniques used in classification showed no statistical significance (>0.05) when compared to ground truth data. The CMRI was observed to have performed better and hence confirmed its sensitivity in estimating mangroves and that other satellite missions with optical sensors and multiple bands can be used to generate the index with high accuracy.

DEDICATION

I dedicate this work to my dear mother, Mrs. Esther Sackey-Addo. Thank your encouragement and sacrifice during my entire research.

ACKNOWLEDGEMENT

I would like to thank the Global Monitoring for Environment and Security & Africa project for funding my entire studies. I would like to express my sincerest gratitude to my supervisors Professor George Wiafe and Dr. Kwame Agyekum for their support. To Mr. Ignatius Williams for the immense support, time, patience, and his impartation of remote sensing skills during my period of work, I say thank you and God bless you. A very big thank you goes to the entire staff of the Global Monitoring for Environment and Security & Africa project for their time, support and assistance offered me during the entire work. I would also like to acknowledge my family members especially Mrs. Joyce Gyasi, colleagues, friends and loved ones for their immense support and encouragement. God richly bless you all. To the entire staff of the Department of Marine and Fisheries Sciences, I express my gratitude for the useful advice during my entire time of study, I am most grateful.

TABLE OF CONTENTS

DECLARATION ii

ABSTRACT iii

DEDICATION v

ACKNOWLEDGEMENT vi

TABLE OF CONTENTS vii

LIST OF FIGURES x

LIST OF TABLES xi

LIST OF ABBREVIATIONS xii

CHAPTER ONE 1

INTRODUCTION 1

1.1 Background 1

1.2 Problem Statement 4

1.3 Justification 5

1.4 General Aim 6

1.5 Specific Objectives 6

CHAPTER TWO 7

LITERATURE REVIEW 7

2.1 Status and Distribution of Mangroves 7

2.2 Mangroves in Ghana 8

2.3 Importance of Mangroves 9

2.4 Threats to Mangroves 10

2.5 Remote Sensing of Mangrove Forests 13

2.6 Techniques of Mapping Mangroves 16

CHAPTER THREE 22

MATERIALS AND METHODS 22

3.1 Study Area 22

3.2 Data Acquisition 23

3.3 Criteria for The Selection of Indices Used in Study 25

3.4 Image Processing 26

3.5 Normalized Difference Vegetation Index (NDVI) 27

3.6 Combined Mangrove Recognition Index (CMRI) 27

3.7 Supervised Classification 29

3.8 Validation and Accuracy Assessment 31

CHAPTER FOUR 39

RESULTS 39

4.1 Normalized Difference Vegetation Index (NDVI) 39

4.2 Combined Mangrove Recognition Index (CMRI) 41

4.3 Supervised Classification 44

4.4 Performance and Validation 45

CHAPTER FIVE 48

DISCUSSION 48

5.1 Mangrove Mapping 48

5.2 Performance of Indices and Supervised Classification 50

CHAPTER SIX 52

CONCLUSION 52

6.1 Conclusion 52

6.2 Recommendation 53

REFERENCES 54

APPENDIX 59

LIST OF FIGURES

Figure 3. 1: Map showing the location of study area.....23

Figure 3. 2: Sentinel-2 imagery of study area clipped into AOI in true colour and false colour 25

Figure 3. 3: Screenshot of AOI overlaid on satellite imagery 26

Figure 3. 4 Screenshot of NDVI map generation in ArcMap using the Raster Calculator spatial analyst tool.....27

Figure 3. 5: Screenshot of CMRI map generation in ArcMap using the Raster Calculator spatial analyst tool.....28

Figure 3. 6: Screenshot of threshold determination to map out mangroves 29

Figure 3. 7: Selected regions used as training samples for supervised classification.....30

Figure 3. 8 Screenshot of validation points taken.....32

Figure 3. 9: UAV imagery overlaid on NDVI map 38

Figure 4. 1: NDVI classification of study area.....39

Figure 4. 2: NDVI map showing mangrove threshold between 0.27 and 0.35.....40

Figure 4. 3: NDWI classification of study area.....41

Figure 4. 4: CMRI classification of study area.....42

Figure 4. 5: CMRI threshold map showing mangroves between the values of 0.5 and 0.7....43

Figure 4. 6: Supervised classification map showing various classes.....44

Figure 4. 7: Supervised (a), CMRI (b), NDVI (c) classification techniques showing mangrove areas in green. UAV imagery (d) of subset area used for validation.....45

Figure 4. 8: Mangrove area coverage of the three classification techniques.....47

LIST OF TABLES

Table 2. 1: Table of some satellite's sensors, spatial resolution, revisit time and the number of bands of each 18

Table 3.1: Table showing description of satellites data used 24

Table 3.2: Multispectral bands of Sentinel-2A 24

Table 3.3:Table showing description of indices used (NIR: Near Infrared) 28

Table 3. 4: Classification Classes and description 31

Table 3. 5: Table showing ground truth points and NDVI interpretations 32

Table 3.6: Table showing ground truth points and CMRI interpretations 35

Table 3.7 Table showing ground truth points and supervised classification interpretations ... 36

LIST OF ABBREVIATIONS

CMRI	Combined Mangrove Recognition Index
IMPA	Indo-Malay-Philippine Archipelago
NDVI	Normalized Difference Vegetation Index
NDWI	Normalized Difference Water Index
RS	Remote Sensing
SR	Simple Ratio
SAVI	Soil Adjusted Vegetation Index
NIR	Near Infrared
OLI	Operational Land Imager
FAO	Food and Agriculture Organisation
GMW	Global Mangrove Watch
LULC	Land use/land cover
UNEP	United Nations Environment Programme
ITTO	International Tropical Timber Organisation
EO	Earth Observation
LiDAR	Light Detection and Ranging
USGS	Geological Survey
TM	Thematic Mapper
ETM+	Enhanced Thematic Mapper Plus
MODIS	Moderate Resolution Imaging Spectroradiometer

NOAA	National Oceanic and Atmospheric Administration
AVHRR	Advanced Very High-Resolution Radiometer
SAR	Synthetic Aperture Radar
LAI	Leaf Area Index
MLC	Maximum Likelihood Classifier
GLCM	Grey-Level Co-Occurrence Matrix
SVM	Support Vector Machine
RF	random forest classification
PCA	principal components analysis
ESA	European Space Agency
SWIR	Short Wave Infrared
AOI	Area of Interest
ROI	Region of Interest
UAV	Unmanned Aerial Vehicle
ESRI	Environmental Systems Research Institute

CHAPTER ONE

INTRODUCTION

1.1 Background

Mangrove forest are unique vegetations that usually grow in areas between land and sea. They are mostly found along the coast, estuaries, tropical and subtropical regions of the world and are uniquely adapted to thriving in soils where there exist conditions of high salinity, and extreme tides (Joshi & Ghose, 2003; Kathiresan & Bingham, 2001). They cover approximately 180,000 km^2 of land coverage accounting for less than 1% of global forests (FAO, 2007; Aheto et al,2011). Mangroves in Africa cover an area of 32,000 km^2 distributed along the coast with the Niger Delta alone supporting 10,000 km^2 mangrove stands in Nigeria. (Ajonina, Diamé, & Kairo, 2018). In Ghana, mangrove vegetation cover approximately 137 km^2 land area, representing less than one percent of area they cover in Africa (Nortey et al, 2016).

Despite their relatively small spatial extent, mangroves are an important resource in coastal and marine ecosystems. They are primary producers and thus serve as food for the other trophic levels. They help in the prevention of coastal erosion by reducing current speed and trapping sediments which help in shoreline stabilization (Lovelock, 1993), they serve as permanent or partial habitats for living organisms including coastal birds, serve as protection against predators as well as nursery and breeding places thereby playing a big role in biodiversity support (Ellison, 2008). The mangrove vegetation plays an important role in helping to curb the effects of climate change as they serve as carbon sinks by trapping excess carbon (Polidoro et al., 2010). In Ghana, the ecosystem is highly valued by coastal communities. They support livelihood by providing goods such as fuelwood and wood for fish tanning and construction.

Coastal communities practice farming activities around the mangrove ecosystem due to the saturated nature of the soil, especially rice production (Dayton et al. 2012).

Mangrove ecosystems are threatened environments despite their ecological and economic importance. Globally, approximately 44% of the population of the world live within the coastal zone within which mangroves are found. The overpopulation of the coastal zone has led to the increase in demand for development and the uses of coastal resources and as a result has led to the extensive clearing of mangroves for these activities (Polidoro et al., 2010). In Africa , the overexploitation of mangroves by activities such as the converting of mangrove areas for agricultural purposes, aquaculture and urbanization, have resulted in observable declines in the area of coverage in the last half century (Armah et al., 2009; Medeiroset et al., 2018). The rate of loss of mangroves continues to be on the increase as the pressures on the ecosystem also increases.

Mangrove ecosystems by nature are difficult to access because of the rough conditions of their surroundings which makes it difficult for field surveys to be carried out by researchers. The use of Remote sensing and Earth Observation (EO) data is now widely used for the mapping of mangrove ecosystems and this has been helpful especially in areas that are inaccessible (Gupta et al., 2018). The spectral signature of vegetation makes it possible for vegetation to be easily identified and mapped out using data obtained from satellites. Vegetation generally have unique spectral range occurring within specific parts of the electromagnetic spectrum which makes it easily classified and separable from other land cover types. Remote sensing applications have evolved due to advancement in technology in combination with historical remote sensing data making it easier to discriminate mangroves. Lately, the advancement in the availability of Remote Sensing and Earth Observation (EO) data, improved methodologies and the development of human resources have made it possible to detect and monitor mangroves not only on local levels but globally and on regular basis. There have been

improvements in the resolution of imageries obtained from various satellite platforms and thus an increase in applications and development of techniques for improved mapping of vegetation.

To distinguish between vegetation and other features, the unique spectral signatures of the vegetation and their morphological characteristics are employed to develop vegetation indices. The Normalized Difference Vegetation Index (NDVI), Normalized Difference Water Index (NDWI), Soil Adjusted Vegetation Index (SAVI), Simple Ratio (SR) are some of the indices generated. NDVI is the most widely used spectral index mainly used for the separation of vegetation from non-vegetation with their spectral reflectance possible to be extracted for analysis. Vegetation of similar spectral reflectance to that of mangroves continue to remain a difficulty in the discrimination of species due to pixel mixing. This usually results in over-estimation or misclassification of mangroves during image processing. However, several vegetation indices have been developed to increase the accuracy of mangrove discrimination from other vegetation. This study seeks to apply and evaluate the performance of the Combined Mangrove Recognition Index (CMRI) in the estimation of mangroves and comparing it to the Normalized Difference Vegetation Index (NDVI) and the supervised classification (maximum likelihood) technique.

1.2 Problem Statement

Mangroves remain an important part of the coastal ecosystem as they have a wide range of importance notwithstanding their small coverage area globally. Despite the numerous benefits and uses of mangroves, the mangrove ecosystem is threatened by natural and anthropogenic pressure. Human activities that have profound influence on mangrove ecosystem some of which include; agriculture, industry, forestry, tourism, housing and human settlements, fisheries, salt and sand winning, disposal of domestic and industrial wastes, dumping of hazardous and unwanted material, and recreation (Sackey et. al, 2011). Due to these factors, the mangrove ecosystem is being depleted at a fast rate. Research carried out by the Global Mangrove Watch (GMW) in 2018 revealed that mangroves declined at a rate of 0.21% between 1996 and 2016 in majority of countries (97%) that possess this important ecosystem. There is therefore an increasing concern to monitor the ecosystem to conserve and make informed management decisions taking advantage of remote sensing and the availability of EO data. The nature of the mangrove ecosystem makes it very difficult for field surveys to be carried out regularly and over a large area. The use of remote sensing technology including various satellite platforms are used to acquire data from these seemingly unreachable areas making it very easy for the ecosystem to be accessed and studied by researchers. There are various techniques by which mangroves can be distinguished from other vegetation and landcover features. A number of vegetation indices have been developed to perform this discrimination by the use of the unique spectral reflectance of mangroves. There is however the problem of mixed pixels between mangroves and other vegetation mostly experienced in areas where mangroves are mixed with other species of vegetation.

1.3 Justification

The role of mangrove forest in the coastal ecosystem is very important and there is therefore the need to examine and monitor mangrove forests periodically. The nature of this ecosystem makes it a laborious task to acquire reliable, accurate and timely data. By employing the labour-intensive field surveying method, it is difficult to accurately map large mangrove forest areas as it will require huge efforts in terms of resources such as time and funds. Remote sensing and Earth Observation (EO) data provides the avenue to overcome this difficulty by the capabilities of various satellite platforms in acquiring information over a large area and more frequently although it does not completely substitute field surveys(Roslani, et al, 2015). A number of studies have been carried out in using satellite imagery for distinguishing among mangroves and other vegetation but the common challenge running along almost all studies has been the difficulty in exclusively separating the mangroves due to the closeness in spectral signatures between the mangroves and other vegetations. This usually leads to the case of over or underestimation of the mangrove coverage area. The Combined Mangrove Recognition Index (CMRI) is useful for distinguishing between mangroves and other vegetation. This study seeks to test its performance compared to the Normalized Vegetation Index (NDVI) and the Supervised classification (maximum likelihood) technique at the Keta Lagoon Complex.

1.4 General Aim

The main aim of this study is to determine the area coverage of mangrove vegetation in the Keta Lagoon Complex, Ghana, using very high-resolution multispectral satellite imagery and test its ability to discriminate mangrove vegetation from other vegetation.

1.5 Specific Objectives

This study specifically seeks to:

1. To test the applicability of the indices NDVI, NDWI and CMRI to mapping the Keta Lagoon Complex, Ghana.
2. Implement supervised classification using NDVI and CMRI to map out the Keta Lagoon Complex.

CHAPTER TWO

LITERATURE REVIEW

2.1 Status and Distribution of Mangroves

Mangrove forests are generally found in tropic and sub-tropic parts of the coastal zone globally where there is the presence of high saline soil with an inflow of fresh and salt water. Mangroves as well as other vegetation that inhabit these areas are adapted to growing in such an environment unlike any other vegetation (Ibharim et al., 2015).

Mangroves are distributed globally across 112 countries within the tropical and subtropical regions. Despite this broad spread, approximately 70% are found in twelve (12) countries with Indonesia accounting for 20% (Spalding et al., 2010). Generally, mangrove forest cover less than 1% of the total area of forests globally. The total area coverage of mangroves in Africa is estimated to be 3.2 million hectares representing about 19% of the global mangrove area coverage (Spalding et al., 2010).

The recorded number of true mangrove species are 70 species globally with about 17 of them found in Sub-Saharan African countries spreading from the coast of Senegal to Congo. (UNEP, 2007). Although West Africa is known to have fewer mangrove species, the riverine nature of the West African coast provides a favourable environment for mangroves to thrive and therefore they are widespread along the west coast than in the east coast (Shumway, 1999). Nigeria has the highest mangrove extent in Africa, spanning 653,669 hectares in area (Giri et al., 2011). Reports suggest that about 19% of mangroves are found in areas that have been designated as protected areas globally (Chape et al. 2005).

2.2 Mangroves in Ghana

The coast of Ghana extends for approximately 550 km (Tsikata et al, 1997) representing about 6.5% of the land area where about 25% of the country's population reside (Amlalo, 2007). The estuaries of major rivers and lagoons have characteristics that help the development and adaptation of mangroves resulting in natural endowment of mangrove resources which are exploited for different purposes by coastal communities. The country's forest area covers about 81,342 km^2 of land area (Gordon and Ayivor, 2003) out of which the area covered by mangroves is estimated to be about 137 km^2 which is only 0.2% of the tropical forest area coverage (UNEP, 2007). The areas in coast of Ghana from the border of Ivory Coast to the areas around Cape Three Points are made up of number of coastal lagoons and estuaries which are favourable conditions for the development of mangroves and hence are found in areas including Half Assini, Amanzure lagoon, Axim, Princes Town and Shama, among others including Takoradi area. In the eastern coast stretching from the Central Region to the Volta Region, they can be found along the Wetlands and lagoons such as the Muni Lagoon, Sakumo-1 lagoon, Korle Lagoon, and in coastal areas including Apam, Winneba, Bortianor, Ada, Sroegbe, and along the Keta lagoon. Mangroves in the eastern coast of Ghana are predominantly found along the delta of the Volta River (UNEP, 2007; Spalding et al, 2010; Gordon and Ayivor, 2003).

There are three species of mangroves known along the coast of Ghana; *Rhizophoran racemose*, *Laguncularia racemose*, and *Avicennia germinans*, commonly known as red, white and black mangroves respectively. *Rhizophora racemosa* are adapted to areas that have moderate soil salinity levels and thus tend to be found along the open lagoons along the coast. *Avicennia germinans, Conarcarpus erectus, Laguncularia racemosa and Acrostichum aureum* are adapted to areas with very high levels of soil salinity and so they are also dominant around the closed lagoons along the coast of Ghana while *Avicennia germinans* which is adapted to a much

lower level of soil salinity are dominant on the landward side coast (UNEP, 2007; Ajonina, 2011).

In the International Tropical Timber Organisation (ITTO) Pre-Project final report by Akpalu (2007), mangroves with relatively high density occurred in the far West and East of the county that is within the Evergreen and Moist Evergreen respectively and the Savanna Ecological Zones with the highest concentration of mangroves in the Savanna zone occurring in the Volta Region. The most developed mangroves in Ghana are found in the western coast of the country between Côte d'Ivoire and Cape Three Points, primarily associated with the extensive lagoons (UNEP, 2007).

2.3 Importance of Mangroves

The essence of mangrove resources to the socio economy of human communities cannot be over emphasized despite their low coverage area. In Ghana, the economic contribution of mangrove related activities and contribution to the marine fisheries sector is valued around $600,000 per annum (Ajonina, 2011; Gordon et al., 2009).

Mangroves continue to be of great value to humanity through a wide range of ecosystem services. Ghana's mangrove ecosystems play a major role in the country's biodiversity. They serve as safe havens for a large number of organisms birds, mammals, amphibians, reptiles, fish and inveterate species. They also serve as habitats, sanctuaries and breeding grounds for migratory bird as well as endangered species. Reports have revealed that inhabitants of coastal areas have used Mangroves for centuries (Luther and Greenburg, 2009). They provide for the direct products harvested from mangrove forests such as prawns, fishes, mud crabs, gastropods, valves and timber (Little, 1980). The wood from mangroves are used for fuel, tanning of fish, for building materials, and also for sale in other communities, generating income and serving

as a means of livelihood for the local community (Gordon and Ayivor, 2003; Spalding et al, 2010, Ajonina, 2011) as seen in Anyanui in the Volta Region Of Ghana where there is a mangrove fuelwood market. Apart from wood, there other essential products produced by mangroves. These include medicines that can be used to treat aliments like tuberculosis and leprosy, and can be used for house thatching in rural communities (Myers, 2016).

Over the past few years, researchers have showed great interest in the studied of using mangroves as an approach to control and reduce natural disasters occurring in the coastal zone that poses threats to land and man (Jan-Willem et al., 2014). The roots of mangroves act like shock absorbs dissipating high energy frequencies resulting from activities in the oceans and well as increasing sediment retention in harsh wave seasons. Ecologically, these mangroves are major contributors to the food chain. Their leaves are converted into detrital materials for the base of a food chain like detritus to worms or worms, then to carnivores like crabs and then humans and the chain goes on and on. In view of this, trophic energy level is sustained due to the secured provision by these mangroves. Other benefits of mangroves include acting as a buffer between the sea and land. As a result of global warming, the land stands chances by being eaten into the sea and these mangroves serves as barriers hence preventing the impact.

2.4 Threats to Mangroves

Mangroves provide a wide range of ecosystem services and goods, a few of which have been highlighted, yet mangrove forests continue to decline and at an alarming rate. According to Duke et al., (2007), mangroves are being lost on the global front at a mean rate 1-2% per year. These figures have been highlighted by Valiela et al, (2001) to be higher than the rate decline of tropical rain forest or coral reefs recorded. There has been a decline of approximately 35% of mangrove forests between 1980 and 2000 (Giri, 2016). There are a number of threats leading

to the decline of the ecosystem of mangroves which need to be seriously considered in order to ensure the conservation of this important coastal resource. Two areas recorded to have shown the greatest rate of loss between the period of 1980-2005 have been the Indo-Malay-Philippine Archipelago (IMPA) with a reduction of 30% and the Caribbean with 24-28% in mangrove (Mckee et al., 2007, Gilman et al., 2008, Polidoro et al., 2010). Polidoro et al, accounted the major reduction of mangroves in the IMPA to the conversion of mangrove habitat for shrimp aquaculture and further held that the Caribbean had its reduction resulting from the increase in coastal and urban development, solid waste disposal, extraction of fuel-wood as well as conversion to aquaculture and agriculture. Spalding et al (2010) reports that with the exception of Australia, all regions have recorded losses of over 20% over a 25year period starting from 1980 to 2005. Their research discovered that over the last three decades, the loss has seen a declining reflective in 1.04% in the 1980s to 0.72% in the 1990s and an even lower loss rate in 2000s at 0.66%. The research highlighted the possibilities of the decline in loss rate as an indication of the increasing resilience of the remaining mangroves or the result of the effective conservation and restoration or rehabilitation efforts. Anthropogenic causes are responsible for mangrove destruction at present, but relative sea-level rise could be the greatest threat to mangroves in the future.

Climate change, particularly sea level rise as mentioned earlier, is without doubt a major threat to the longevity of mangroves. Schleupner, 2008 holds that mangrove areas most vulnerable to sea level rise are believed to be those of low-relief carbonate islands with low rate of sediment supply and little available upland space. Osland et al., 2014 adds that in addition to this are mangroves in arid, semi-arid and dry sub-humid regions. On the other hand, it has been posited by Ellison and Zouh, 2012 that macrotidal coastlines (>4m tidal amplitude) with significant riverine inputs are least vulnerable. Irrespective of the opposing views on the extent of and the nature of the effect of climate of climate change drivers on mangroves, there is a general

agreement on the position that the vulnerability of mangrove forests is increased by the occupation and urbanization of the coastal zone as well as the conversion of mangrove areas to other land uses (Soares, 2009). Some recent studies have however explored the possibility of some of the other effects of climate change on the mangrove ecosystem. Gilman et al., (2007) have held that increased precipitation, temperature and atmospheric carbon ($C0_2$) concentration actually may increase mangrove productivity.

In Ghana, the decline of mangroves cannot be said to be absent. Despite the small area covered by mangroves in the country, they are still threatened. It has been recorded that the country lost about 24% of its mangrove forest between 1980 and 2006 (Henry,2016). The most prevalent threat to mangroves is the increase in population in the coastal zone of the country. The migration of a large number of the population of Ghana to the zone eventually leads to the over exploitation and the ultimately the conversion of mangrove ecosystems into other land uses, mostly development of urban centres and industry; engineering in the rivers and coasts such as the construction of dams and sea walls; and land-based sources of marine pollution in order to satisfy the needs of the growing population (UNEP, 2007). Lawson (1986) reported the use of about half of the area previously occupied by mangroves near the mouth of the Densu River near Accra for salt production. A report by Sackey (1994) also indicated that indiscriminate harvesting of mangrove wood and garbage dumping was widespread in the Iture estuary, located in the Central Region of Ghana and these activities were likely to have profound effect on the structure and productivity of the mangrove vegetation.

In trying to conserve the mangrove ecosystem in Ghana, the approach of community-based coastal management principles and traditional management efforts have been applied. A number of non-governmental agencies such as the USAID have carried out a number of mangrove restoration projects and mangrove coverage area studies all with the aim of protecting the ecosystem. In addition to these efforts, five Ramsar sites in the central and

eastern parts of the country, which include mangrove habitats, have been designated since 1992 (Spalding et al, 2010; UNEP, 2007). These Ramsar sites are managed for sustainable conservation, the ecosystem is however still over- exploited (Spalding et al, 2010). There is however not a single body soles responsible for the conservation of mangroves in the country. Different government agencies, for example the Environmental Protection Agency (EPA), Forestry Commission and non-governmental organizations perform activities that border on mangroves and biodiversity as well as their conservation and management in general (UNEP, 2007).

2.5 Remote Sensing of Mangrove Forests

The application of Remote Sensing (RS) and Earth Observation (EO) data have been widely used in recent times to monitor and map vegetation including mangroves from their distribution to ecosystem parameters and inventory (Wang et al., 2019). A wide range of data can be acquired from different sensors on different platforms. This may range between multispectral and hyperspectral sensors which are able to sense data of different wavelengths, that is from the visible wavelength, perceivable by the human eye, to the microwave wavelength. Various data obtained from satellites may have different spatial resolutions and also different frequencies at which data may be accessed and be available depending on the type of sensors. Some satellites have a shorter revisit time ranging from days to months, as well as different resolutions at which the data obtained comes and they are able to acquire data over a large area which makes the use of satellites more advantageous over field survey techniques (Thomas et al., 2018).

Naturally, the environment in which mangroves are found, that is areas of saturated saline soils, mostly around wetlands with bodies of water make it very difficult for research to be carried out and also, only a small area can be covered at a time. Remote Sensing technology over a

few decades has made it possible for these unique habitats to be studied efficiently, repetitively and over a large area. Data obtained from Earth Observation sources, that is satellite imagery have been on the increase over the past few years with studies such as the mapping of mangroves globally, the area coverage of mangroves in domestic and regional domains, the determination and estimation of carbon that is stored by mangroves, study of biophysical characteristics, and in very recent times, the identification and mapping of mangrove species, just to mention a few (D. Wang et al., 2018). In the early days of the introduction of remote sensing, the availability of data and the know-how of the use of satellite imagery was quite a challenge, but in recent times, remote sensing has seen a major improvement in the availability of data, most of which can be freely accessed over the internet by agencies such as the European Space Agency that offers the Sentinel series satellite data under the Copernicus programme and the LANDSAT imagery from the United States Geological Survey (USGS) accessible all over the world at regular basis with improved data quality and processing methodologies as well as human skill (Giri, 2016).

Important information and a lot of them at that, for example the retrieval of information from the leaf pigments such as chlorophyll a, b, and nitrogen concentrations (Pham et. al, 2019), can be obtained from a simple satellite image. The information acquired may be used to study or determine the rate at which vegetation, or specifically mangroves are being declined and what factors are causing the decline by the generation of land use land cover maps, the study of how healthy a mangrove population is, the evaluation of the abundance of mangroves present at a particular area, the amount of carbon stored by these mangroves; all of these information can be extracted and produced over large areas and at any time making the use of this form of data a very reliable and time saving source for making informed decisions on the conservation and management of this important resource(Kuenzer, Bluemel, Gebhardt, Quoc, & Dech, 2011).

In the mapping of vegetation using remote sensing and Earth Observation data, spectral characteristics of vegetation are used. The chlorophyll in the leaves of plants have a high radiation usually in the red and near-infrared portion of the electromagnetic spectrum. This is taken advantage of by using them in the generation of vegetation indices which clearly delineates them from other land cover features (Asrar et al. 1984; Galio et al. 1985). These differences in the spectral reflectance of vegetation enable the study of a number of parameters and information some of which have been mentioned earlier (Beeri et al. 2007). In the use of satellite imagery, the resolution of the imagery obtained to be used in analysis is very important. In the early days of Remote Sensing technology, the resolution of data obtained from optical sensors made them difficult for accurate classification analysis, but in recent times, there has been tremendous improvement in image resolution (spatial and spectral) through the launching of new optical satellite missions such as the Sentinel-2 and also the development of multispectral and hyperspectral sensors, coupled with the use of Unmanned Aerial Vehicles (UAV) which are able to now acquire up to about less than 5cm of image resolution (Giri, 2016).

Different satellite sensors have different spatial, temporal, spectral and radiometric characteristics, which make the selection of the appropriate sensor a very important factor to consider when mapping vegetation. The selection of images acquired by adequate sensors is largely determined factors such as the mapping objective, the cost of images, the climate conditions and the technical issues for image interpretation (Xie, Sha, & Yu, 2008). The mapping objective of a study involves what is to be mapped and what mapping accuracy is expected. Images with low resolutions may be used when the high level of vegetation classes are to be identified, while the images with relatively higher resolutions are used for fine-detailed classifications of vegetation. Remote sensing imagery may be very expensive and the cost of imagery is definitely a consideration when choosing imagery. From the mapping scale

point of view, vegetation mapping at a small scale usually requires high-resolution images, while low resolution images are used for a large-scale mapping. However, in recent times, satellite data have been made freely available globally for example LANDSAT imagery from the United States Geological Survey (USGS) and the European Union Copernicus programme sentinel satellites. Again, some technical specifics need to be taken into account regarding image quality, pre-processing and interpretation when choosing suitable sensors. The most commonly applied sensors include Landsat (mainly TM and ETM+), SPOT, MODIS, NOAA–AVHRR, IKONOS, QuickBird and Sentinel(Xie et al., 2008).

2.6 Techniques of Mapping Mangroves

The mangrove ecosystem plays a big part in the general coastal ecosystem and therefore forms an integral part of the coastal zone which need to be well managed and conserved globally. This can be done by continuous study of the ecosystem in order to learn about any new development (Xiao et al. 2004). Mapping of mangroves involves the collection and analysis of information and data from the ecosystem for the quantification and observation of cover over an area at a given time or over some time. It is important to know the state of vegetation especially in critical areas where there is much decline continuously in order to develop the appropriate programs of restoration (Egbert et al. 2002; He et al. 2005). The techniques for mapping mangroves involve the use of data or imagery obtained from various sensors. The data used may be optical which include multispectral and hyperspectral imagery, Synthetic Aperture Radar (SAR) imagery, or a combination of these data sets (Thomas et al., 2018).

In the classification of mangroves, the spectral signature of mangroves makes it easier for them to be distinguished from other land cover types. Mangroves show higher reflectance in the visible red, near infrared and the mid-infrared spectral ranges on the electromagnetic spectrum.

Over the past few years, there have been improvement in data obtained from remote sensing with improvement in the spatial, spectral and temporal resolution of satellite imagery as well as access to historical data making it possible to improve upon the mapping of mangroves(Giri, 2016). Satellite missions such as the Sentinel-2, World View and Landsat-7 have made it possible for the acquisition of imageries with resolutions of about two metres. The improvements in the resolution of images increases the accuracy of analysis that is carried out using these data sets. In the mapping of mangroves, the techniques that have been used over the years are basically the unsupervised, supervised and a fusion of both. Unsupervised classification method such as the ISODATA technique involves the

The techniques used to detect and delineate mangroves have primarily involved unsupervised classification techniques such as the ISODATA approach, supervised classification techniques such as the maximum likelihood classification (MLC), random forest classification (RF), or other techniques commonly available in commercial image processing software, or a fusion of unsupervised and supervised classification. Other common approaches for the classification of mangroves using multispectral imagery include pre-processing steps such as spectral transformations such as principal components analysis (PCA), Tassel-Cap Transformation, spectral vegetation indices such as Normalized Difference Vegetation Index (NDVI) or Simple Ratio (Heumann, 2011). In the mapping of mangroves, the resolution of the remote sensing data or imagery used, that is the size of a pixel on the ground (for example 10 x 10), is a very important factor to consider. Mangroves are often found or associated with other vegetation where the spectral reflectance of these vegetation are often similar to that of mangroves making it difficult to delineate these features with very high accuracies. However, as mentioned earlier, in recent times, there have been improvements in the technology of sensors which is evident in the improvement of the resolution of satellite imagery and also the improvement in the

methodology used in mapping of mangroves. Table 2.1 shows some common satellite sensors with their spatial resolution, number of bands and their revisit time.

Table 2. 1: Table of some satellite's sensors, spatial resolution, revisit time and the number of bands of each

Sensor	Spatial Resolution	Revisit Time	Number of Bands
IKONOS	4m	3 days	5
SPOT 6 & 7	1.5m, 6m & 10m	1 day	5
MODIS	250m, 500m &1000m	1 to 2 days	36
NOAA-AVHRR	1100m	1 day	5
Landsat 8 TM	15m, 30m & 100m	16 days	11
Sentinel-2	10m, 20m & 60m	2 to 3 days	13

In mapping mangrove forests, it is important to know and understand the importance of the spectral reflectance emitted by chlorophyll cells in the leaves of the mangroves in correlation with their biophysical characteristics when suing multispectral satellite imagery. Satellite imageries of spatial resolutions ranging from low to high very high have been used for a number of mangrove mapping studies. These sensors include MODIS, Landsat TM, Sentinel-2, QuickBird, just to mention a few, as seen in table 2.1. When the resolution of the satellite data is higher, there is higher accuracy in mapping, for example in case of Leaf Area Index (LAI) of mangrove studies (Pham et. al, 2019). Roslani et al. (2015) carried out a study which capitalised on the unique spectral reflectance of mangroves to delineate among mangroves species. This study was carried out using the RapidEye satellite data coupled with the use of the Maximum-likelihood (MLC) classification algorithm. About eleven (11) species of mangroves including *Rhizophora mucronata, Rhizophora apiculata, Bruguiera parviflora,*

Bruguiera cylindrica, Bruguiera gymnorrhiza, Avicennia alba, Avicennia officinalis, Sonneratia alba, Sonneratia caseolaris, Sonneratia ovata and Xylocarpus granatum, were identified with an accuracy of 84% and kappa statistic of 0.8016. The study showed the importance and the capability of using high resolution imagery in mangrove forest mapping, revealing however that the red edge band enhances the classification and also pointed out that it was challenging due to the natural environment pf mangroves with the associated vegetation reducing classification accuracy.

Ke et. al (2010) classified mangrove forest using a mix of data, spectral and Light Detection and Ranging (LiDAR). In this study, it was proven that a mix of data sets yields more classification accuracy as compared to the use of the data individually. The introduction of the LiDAR data was helpful in the enhancement of class separation, a problem caused due to the displacement of relief features on spectral images. Huang et al., (2009) carried out research using IKONOS imagery to discriminate mangrove species. In this study, it was revealed that the use of multispectral imagery in mangrove species mapping is very important as the accuracy reported was 91.4%.

This study however seeks to take advantage of the spectral responses of mangroves by employing the use of vegetation indices such as NDVI and Combined Mangrove Recognition Index (CMRI) to accurately map out mangroves from other vegetation. Image processing included application Normalized Difference Vegetation index (NDVI) and the Combined Mangrove Vegetation Index (CMRI) algorithms, both of which are unsupervised techniques of classification to map out each study site. NDVI when applied on a multispectral image results in the generation of an image which displays the amount of greenness in vegetation. Plant materials have high reflectance in the near-infrared (NIR) band while the pigment of chlorophyll in plants reflects highest in the red band of multispectral satellite images. NDVI values range between -1 and 1 where values close to 1 denotes the presence of green vegetation,

and values from 0 and closer to -1 indicate areas of no vegetation (Alonso, Muñoz-Carpena, Kennedy, & Murcia, 2016). The application of NDVI can be seen in agriculture where it can be used to predict production, it can be used in the monitoring of drought and in this study, it was used in the mapping of mangroves.

The Combined Mangrove Recognition Index (CMRI) combines outputs from NDVI and Normalized Difference Water Index (NDWI) to map out mangrove areas (Gupta et al., 2018). To obtain the CMRI, water classification index NDWI and NDVI was applied on the image. Supervised classification where the user selects representative samples for each land cover class was also carried out in this study. These sample land cover classes are called training data. The classification of land cover is based on the spectral signature defined in the training set. The digital image classification software determines each class on what it is similar to most in the training set. Supervised classification technique enables the image analyst to decide on the classes and specify the training areas of interest to be used for analysis. This method of classification is used to cluster pixels in a data set into classes corresponding to user defined training areas. The maximum-likelihood classification (MLC) algorithm was applied and a landcover map was generated for a sub-set of the Keta Lagoon Complex. MLC assumes that the statistics for each class in each band are normally distributed and then calculates the probability that a given pixel belongs to a specific class. MLC defines the means and variances of the classes from training samples, and then, those are used to compute the probabilities of belonging to a certain class for every pixel in the satellite image (Petropoulos et al. 2012). MLC assumes that the statistics for each class in each band are normally distributed and then calculates the probability that a given pixel belongs to a specific class.

The Cochran's Q and the McNemar tests were used to carry out statistical analysis for the study. This test is used when the observations in an experiment, results are expected to fall between two mutually exclusive values, often coded as "1" for success and "0" for failure, from

which the p-value is then calculated. In this study, the presence of mangroves in each imagery was represented by “1” and non-mangrove for “0”(Sheskin, 2003; UM, 2016). It is calculated as follows:

$$Q = k(k-1)\frac{\sum_{j=1}^{k}\left(x_j - \frac{N}{K}\right)^2}{\sum_{i}^{b} x_i(k - x_i)}$$

(Cochran, 1954)

The following assumptions are considered:

- The sample of n subjects has been randomly selected from the population it represents;
- The scores of subjects are in the form of a dichotomous categorical variable (either "0" or "1").

CHAPTER THREE

MATERIALS AND METHODS

3.1 Study Area

The area for this study is the Keta Lagoon Complex, located in the Volta Region of Ghana. The region forms part of the Volta River estuary which has an open lagoon and an extensive stretch of mangrove forest. The Keta Lagoon Complex is located in the south-eastern coastal belt of Ghana which falls within the Dry Tropical Equatorial climatic region (Yidana et al., 2010). The area experiences the dry and wet seasons annually with an annual mean rainfall of 783 mm and evaporation of 1964mm (Lamptey et al., 2013). The wet season however is usually experienced in two periods; a major rainy season from May to July and a minor rainy season between September and November (Lamptey et al., 2008). The dry season starts In January and ends in March. The recorded average temperature of the area ranges between 24 °C and 31 °C, with a relative humidity varying around 95% at night and morning and 65% during the day (Sorensen et al., 2003). There is an extensive cover of mangroves in this area with *Rhizophora* being the dominant species (Akpalu, 2007). The dominant economic activities in the area include; salt production, fishing, farming of vegetables, salt extraction and the harvesting of mangroves for fuelwood. There is however the threat of over-exploitation of mangroves as they are mostly not replanted after harvesting.

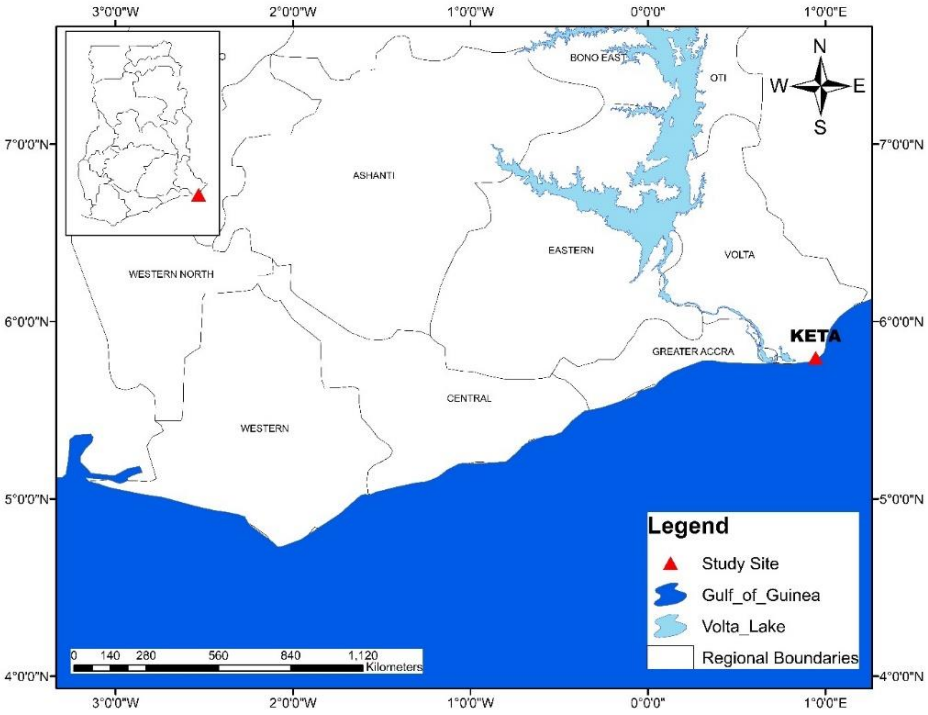

Figure 3. 1: Map showing the location of study area

3.2 Data Acquisition

The satellite data used for the study was Sentinel-2 level-2A imagery was acquired for free from https://scihub.copernicus.eu.com, an open data source of the European Space Agency (ESA) Copernicus programme. The Sentinel-2 is a twin satellite, that is 2A and 2B 180° to each other with a revisit time of two to five days and a resolution of 10m, 20m and 60m. Figure 3.2 shows the true colour and false colour Sentinel-2 imagery of study area. The data is available to users in Level-1C or 2A product types, where measurements are provided in Top of Atmosphere (TOA) reflectance and Bottom of Atmosphere (BOA) respectively. The Level-2A are already pre-processed and thus does not need further pre-processing when downloaded and that informed the choice of the type of Snetinel-2 data used for this study. Table 3.1 shows

the best available imagery with the least cloud cover of the study site. Table 3.2 shows the multispectral bands, the wavelength and the spatial resolution of the Sentinel-2 satellite data.

Table 3.1: Table showing description of satellites data used

Sensor	Date of Acquisition	Number of Bands	Resolution
SENTINEL-2-MSI-MultiRes-UTM 31N	25-DEC-2018	13	10m

Table 3.2: Multispectral bands of Sentinel-2A

Band	Name	Wavelength/(nm)	Spatial Resolution/(m)
1	Coastal aerosol	443.9	60
2	Blue	496.6	10
3	Green	560	10
4	Red	664.5	10
5	Vegetation Red Edge	703.9	20
6	Vegetation Red Edge	740.2	20
7	Vegetation Red Edge	782.5	20
8	NIR	835.1	10
8A	Narrow NIR	864.8	20
9	Water vapour	945	60
10	SWIR – Cirrus	1373.5	60
11	SWIR	1613.7	20
12	SWIR	2202.4	20

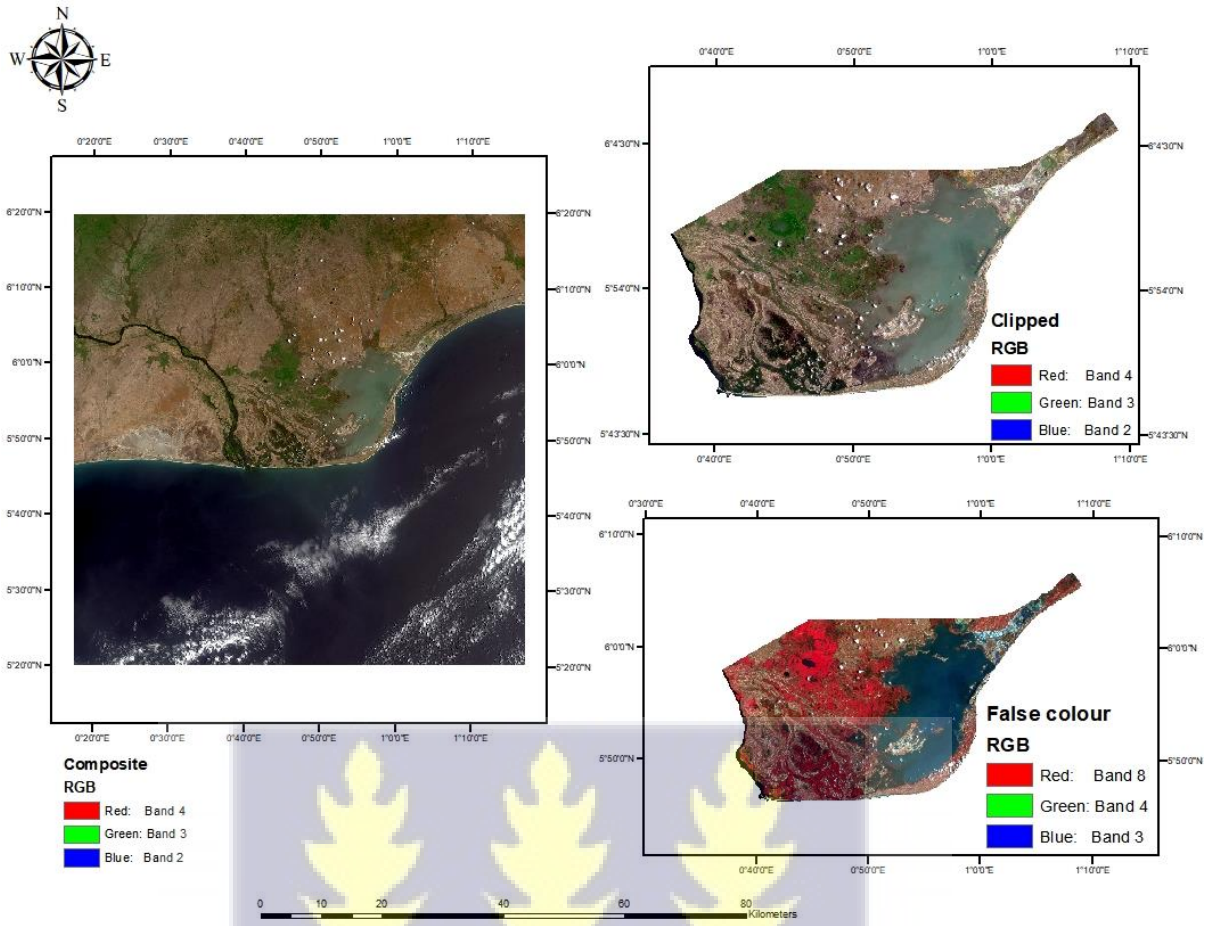

Figure 3. 2: Sentinel-2 imagery of study area clipped into AOI in true colour and false colour

3.3 Criteria for The Selection of Indices Used in Study

NDVI is a widely used and proven technique by which vegetation are monitored using remotely sensed data. The area for this study was the Keta Lagoon Complex With NDVI values being between +1 and -1, the method of thresholding in distinguishing between vegetation and other features is more applicable (Hashim, Abd Latif, & Adnan, 2019). The values close to 1 are areas of vegetation while values closer to -1 are non-vegetation features and water. This therefore makes the index much suited for this study due to the fact that we want to delineate areas with mangrove cover. The CMRI is an index developed to map out mangroves specifically by the combination of NDVI and NDWI used to generate values which delineates

mangroves from other vegetation (Gupta et al., 2018). This index reduces the error in the over estimation of mangrove area coverage and thus suitable for the study. The application of supervised classification in the monitoring of vegetation has been proven to produce accuracies of over 80% (Abd Latif et al., 2012). This classification technique enables the analyst with basic knowledge of an area to select areas of interest to generate land cover maps. The index allows analyst to have control over classification classes and thus was selected for the study.

3.4 Image Processing

The satellite image downloaded extended beyond the Area of Interest (AOI) thus sub-setting was performed. This was done by clipping the AOI using an ESRI shapefile of the actual study site on the satellite image tile, enclosing the area. The resulting image which now covered only the area of interest was then used for image processing as shown in figure 3.3.

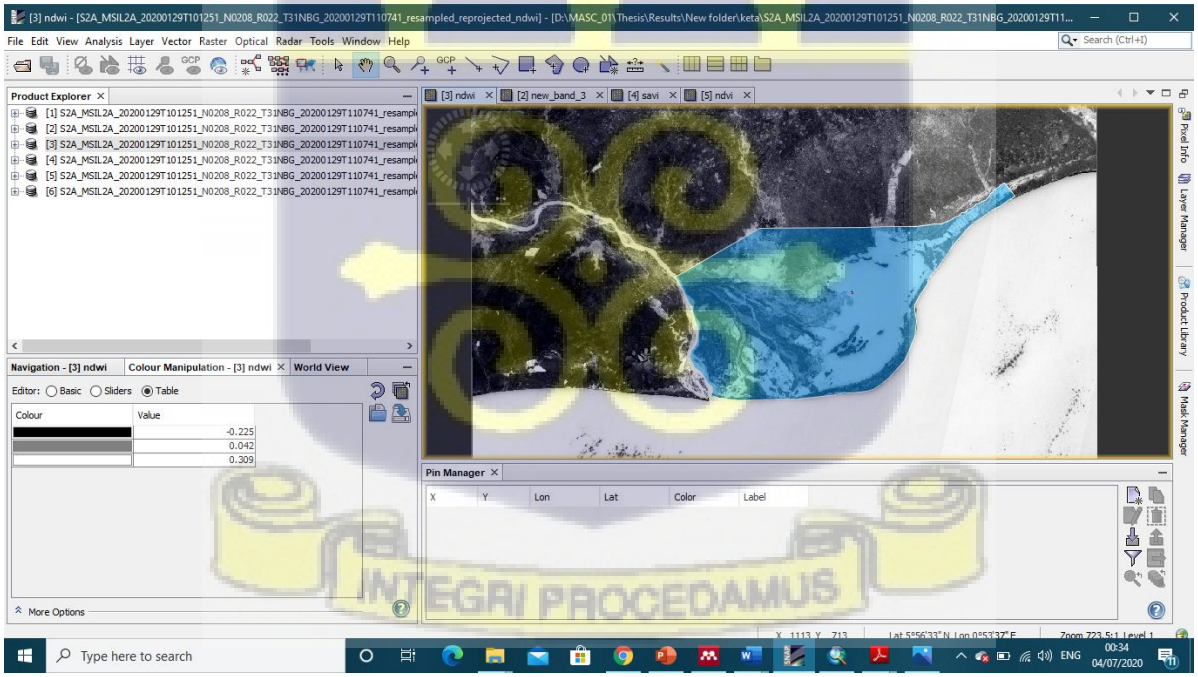

Figure 3. 3: Screenshot of AOI overlaid on satellite imagery

3.5 Normalized Difference Vegetation Index (NDVI)

Normalized Difference Vegetation Index (NDVI) map was generated in ARCMAP using the near infrared (NIR) and red band. Table 2 shows the formula and the bands used for the NDVI. This was done by using the raster calculator tool, as shown in figure 3.4, in which the formula was after inputted to generate the map after which a colour ramp was applied to clearly show the areas and their corresponding NDVI values. Density Slicing was then used to create thresholds, which were used to map out mangrove areas and a colour assigned to the area.

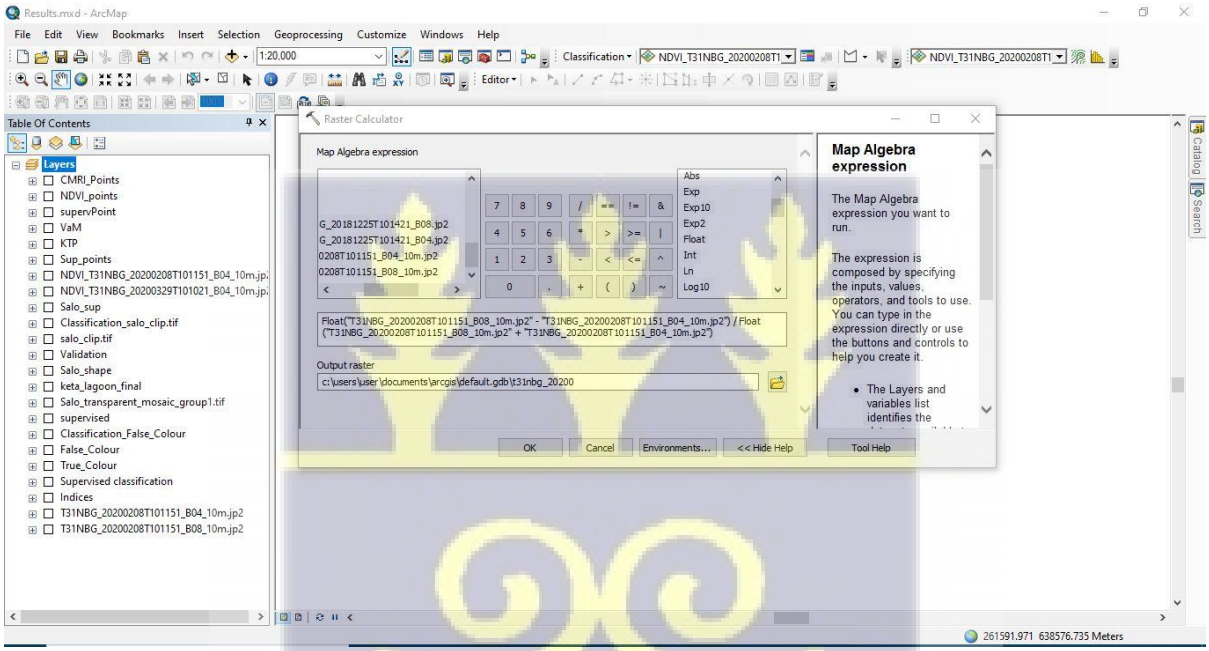

Figure 3. 4 Screenshot of NDVI map generation in ArcMap using the Raster Calculator spatial analyst tool

3.6 Combined Mangrove Recognition Index (CMRI)

To generate the Combined Mangrove Recognition Index (CMRI), a combination of Normalized Difference Water Index(NDWI) and NDVI is used (Gupta et al., 2018). The NDWI map was generated using the Raster Calculator tool, similar to the process involved in generating the NDVI map but this time makes use of the green and NIR, that is bands 3 and 8

respectively. The CMRI map was then generated by subtracting the NDWI from the NDVI as shown in figure 3.5. Table 3.3 shows the description of the formula used to generate the CMRI. Density slicing was again applied to clearly distinguish mangrove areas by the use of threshold values.

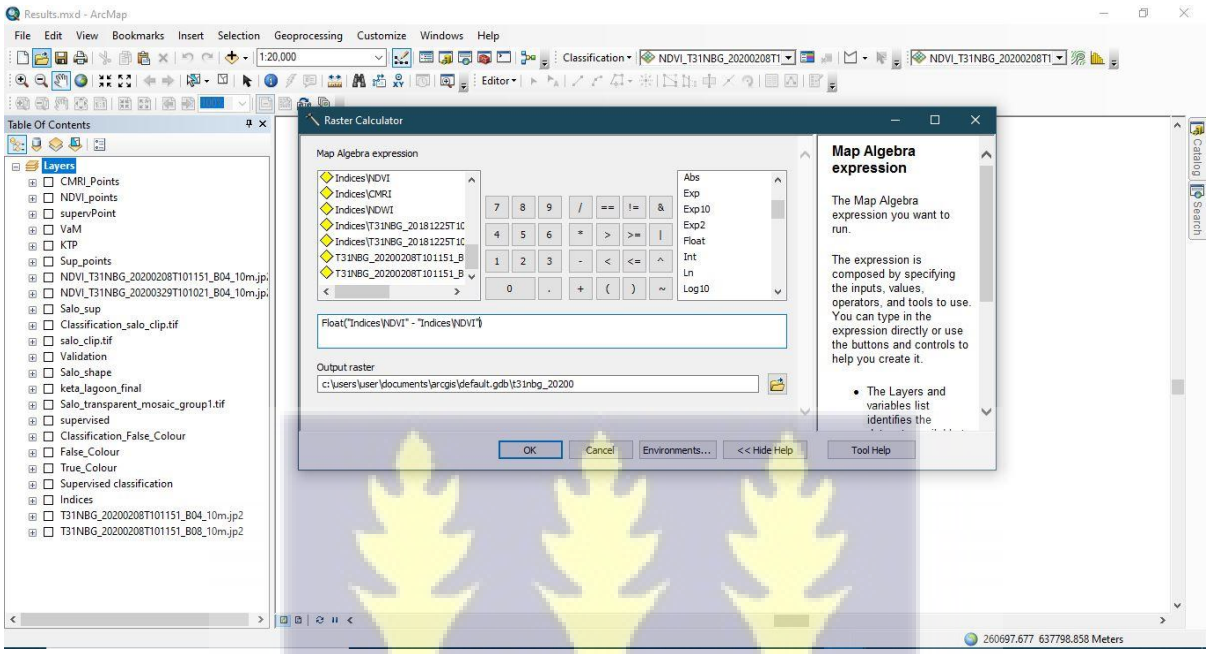

Figure 3. 5: Screenshot of CMRI map generation in ArcMap using the Raster Calculator spatial analyst tool

Table 3.3:Table showing description of indices used (NIR: Near Infrared)

Index	Formula
Normalized Difference Vegetation index (NDVI)	$\frac{NIR -}{NIR +}$
Normalized Difference Water Index (NDWI)	$\frac{-NIR}{+NIR}$
Combined Mangrove Recognition Index (CMRI)	$NDVI - NDWI$

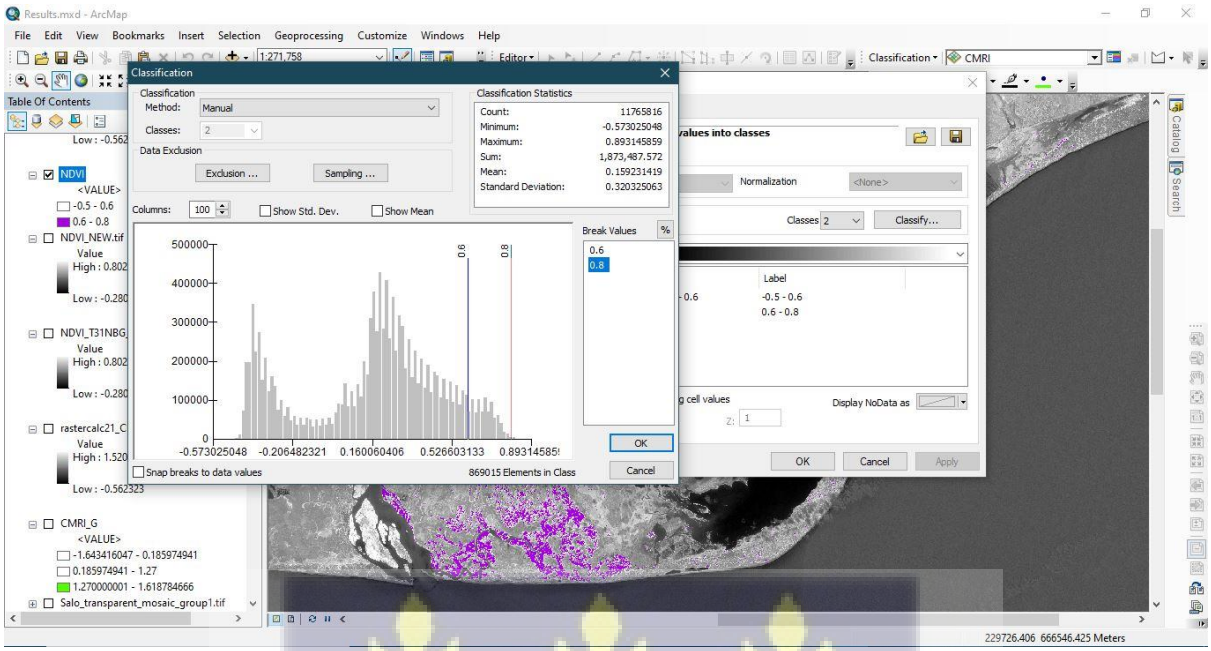

Figure 3. 6: Screenshot of threshold determination to map out mangroves

3.7 Supervised Classification

The initial processing for the supervised classification involved; stacking of layers. This was performed through the combination of different bands to produce suitable imagery for the analyst. Different satellite products have different band combinations and for Sentinel-2 and this study, the true colour and false colour combinations were used. The bands for true colour and false colour for sentinel-2 are 4-3-2 and 8-4-3 respectively as shown previously in figure 3.2. The true colour is the combination easily observable by the human eye, however in this study, the false colour was also used because mangroves show high spectral reflectance in the NIR band. Generally, plants are perceived as green by the human eye because they reflect wavelengths in the green region of the electromagnetic spectrum, however there is high reflectance in the NIR region which cannot be perceived by the human eye but is able to be

sensed by satellites. A plant with more chlorophyll reflects more NIR energy and thus scientists are able to analyse a plants spectrum of reflection and absorption to detect differences in vegetation species. Different regions of areas of interest were carefully selected as training areas as seen in figure 3.7 using the ArcMap base map as a guide. The maximum-likelihood classification (MLC) algorithm, which uses the means and variances of the classes from training samples to compute their probabilities of belonging to a certain class for every pixel in the satellite image (Petropoulos et al. 2012) was applied and a landcover map was generated for the Keta Lagoon Complex. The resulting map was then clipped to the area of UAV imagery used for validation and accuracy assessment. The classification scheme that was used is presented in Table 3.4.

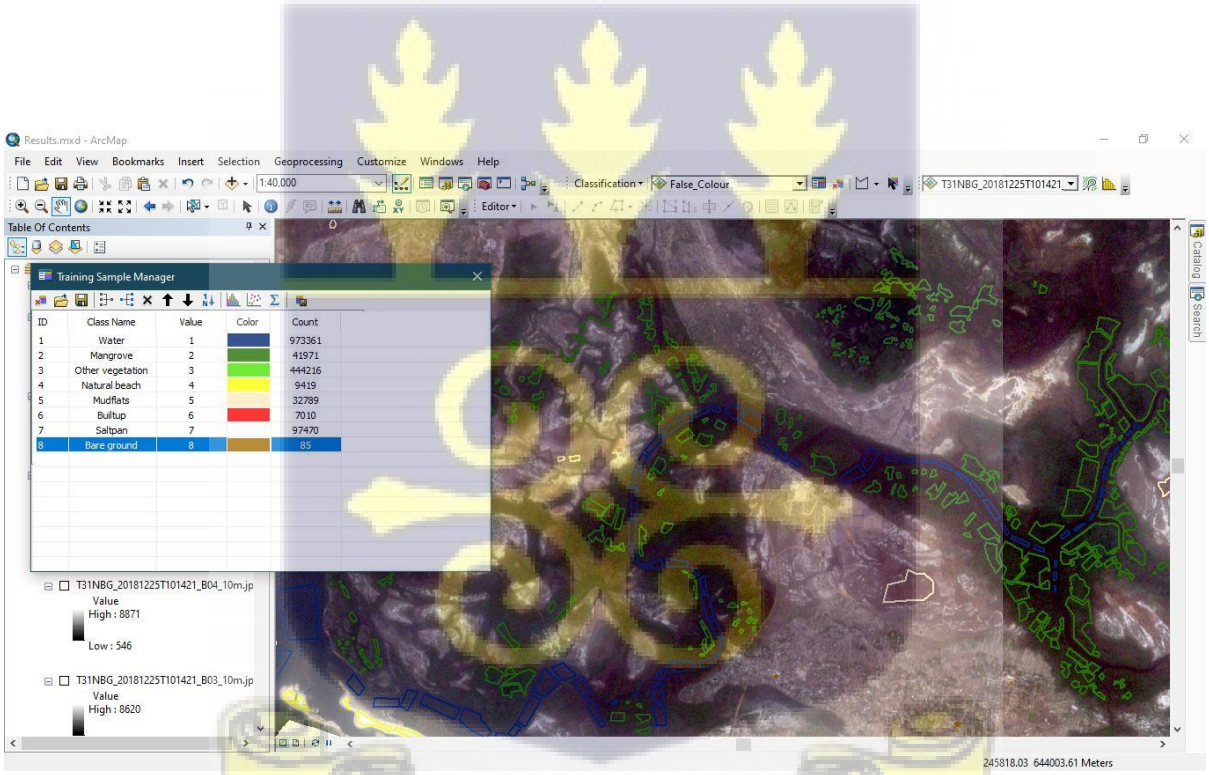

Figure 3. 7: Selected regions used as training samples for supervised classification

Table 3. 4: Classification Classes and description

CLASS	DESCRIPTION
Mangroves	Areas of mangroves, including sparse or dense distribution
Water	Include all water bodies and water related features (including saltpans)
Other Vegetation	Any other vegetation apart from mangroves (grassland, agricultural lands, mangrove associated vegetations, etc.)
Built-up	Include areas of urban development with or without some vegetation (buildings, roads, etc.)
Muddy Areas	Areas of swamps, marshes, mud
Bare ground	Areas with minimum or no vegetation cover
Natural Beach	Areas with beach sediments along the coastline
Salt pan	Areas for salt production

3.8 Validation and Accuracy Assessment

UAV imagery was used for validation by selecting 50 random points from the imagery. These points were overlaid on the NDVI, CMRI and supervised classification maps clipped to the size of the UAV imagery and the interpreted values for each recorded in a table. The areas with mangroves present were assigned the number "1" and the areas that were non-mangroves assigned the number "0". The data from this table is used to find the p-value calculated using the Cochran's Q test as a result of the nature of data (binary data).

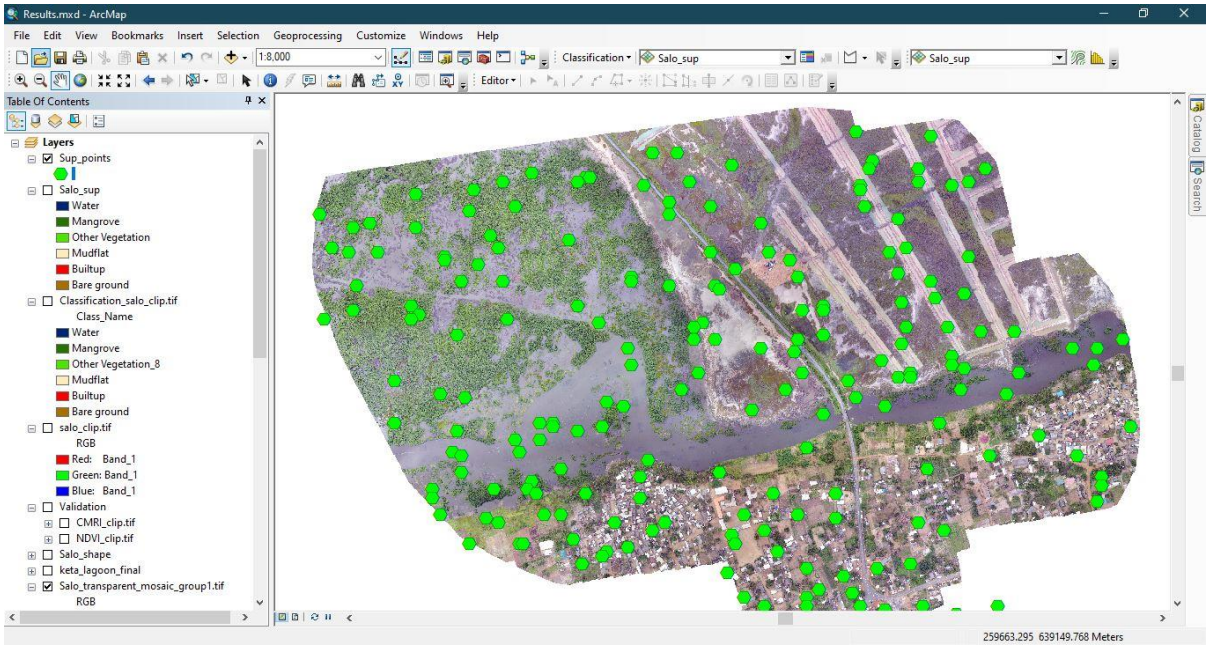

Figure 3. 8 Screenshot of validation points taken

Table 3. 5: Table showing ground truth points and NDVI interpretations

			Ground truth		NDVI	
Site	Lon	Lat	Feature	Interpreted value	Value	Interpreted Value
1	0.821402006	5.78359591	Mangrove	1	0.3559	1
2	0.823438401	5.77958434	Non-mangrove	0	0.2795	1
3	0.82774594	5.77963039	Non-mangrove	0	0.1046	0
4	0.83077422	5.78250859	Non-mangrove	0	0.0914	0
5	0.82835864	5.78535118	Non-mangrove	0	0.1181	0
6	0.827625732	5.78406315	Non-mangrove	0	0.1135	0
7	0.828668589	5.78146655	Non-mangrove	0	0.2967	1
8	0.828434824	5.78858757	Non-mangrove	0	0.0995	0
9	0.824929027	5.78709677	Mangrove	1	0.3038	1
10	0.83548739	5.78455136	Non-mangrove	0	0.0764	0
11	0.83565303	5.78188772	Non-mangrove	0	0.1035	0
12	0.835117521	5.78137011	Non-mangrove	0	0.1473	0
13	0.832540248	5.78017736	Non-mangrove	0	0.1409	0
14	0.827136047	5.78180232	Non-mangrove	0	0.1012	0
15	0.819716377	5.78477973	Mangrove	1	0.3456	1
16	0.8190898	5.78389057	Mangrove	1	0.3613	1
17	0.82058783	5.7814515	Non-mangrove	0	0.1482	0
18	0.823587318	5.78264535	Non-mangrove	0	0.1032	0
19	0.821840478	5.77995167	Non-mangrove	0	0.1821	0

20	0.822391664	5.78675109	Mangrove	1	0.3322	1
21	0.820136902	5.78715852	Mangrove	1	0.3498	1
22	0.818849597	5.78703307	Mangrove	1	0.3548	1
23	0.822172967	5.78071862	Mangrove	1	0.3005	1
24	0.824265409	5.78416566	Mangrove	1	0.3143	1
25	0.831918074	5.78572632	Non-mangrove	0	0.1093	0
26	0.833041529	5.78297655	Non-mangrove	0	0.0817	0
27	0.821732849	5.78716466	Mangrove	1	0.3589	1
28	0.820777118	5.78448822	Mangrove	1	0.3460	1
29	0.826093941	5.78657715	Non-mangrove	0	0.1273	0
30	0.829474834	5.78629451	Non-mangrove	0	0.1054	0
31	0.82476146	5.78000436	Non-mangrove	0	0.1523	0
32	0.819211307	5.7844697	Mangrove	1	0.3591	1
33	0.81930449	5.78651584	Mangrove	1	0.3152	1
34	0.823833584	5.7880015	Mangrove	1	0.3268	1
35	0.8230858	5.78704423	Mangrove	1	0.3297	1
36	0.832209345	5.78241857	Non-mangrove	0	0.1465	0
37	0.835205112	5.78236578	Non-mangrove	0	0.1244	0
38	0.835402849	5.78096249	Non-mangrove	0	0.1234	0
39	0.830398642	5.78827563	Non-mangrove	0	0.0937	0
40	0.825915722	5.77929711	Non-mangrove	0	0.1211	0
41	0.826069711	5.78029018	Non-mangrove	0	0.1246	0
42	0.827217109	5.78078684	Non-mangrove	0	0.2105	0
43	0.827865261	5.78123156	Non-mangrove	0	0.1632	0
44	0.826388915	5.77963259	Non-mangrove	0	0.1598	0
45	0.82406243	5.78039959	Non-mangrove	0	0.3036	1
46	0.821676171	5.78165804	Non-mangrove	0	0.1431	0
47	0.823489169	5.78219023	Non-mangrove	0	0.1124	0
48	0.820135618	5.7858642	Non-mangrove	0	0.1793	0
49	0.822283651	5.78605605	Mangrove	1	0.3396	1
50	0.822198149	5.78452096	Mangrove	1	0.3456	1

			Groundtruth		CMRI	
Site	Lon	Lat	Feature	Interprated value	Value	Interprated Value
1	0.821402	5.783596	Mangrove	1	0.6557	1
2	0.823438	5.779584	Non-mangrove	0	0.5306	1
3	0.827746	5.77963	Non-mangrove	0	0.2586	0
4	0.830774	5.782509	Non-mangrove	0	0.1772	0
5	0.828359	5.785351	Non-mangrove	0	0.2635	0
6	0.827626	5.784063	Non-mangrove	0	0.2455	0
7	0.828669	5.781467	Non-mangrove	0	0.5701	1
8	0.828435	5.788588	Non-mangrove	0	0.2271	0

9	0.824929	5.787097	Mangrove	1	0.5728	1
10	0.835487	5.784551	Non-mangrove	0	0.1536	0
11	0.835653	5.781888	Non-mangrove	0	0.2351	0
12	0.835118	5.78137	Non-mangrove	0	0.3088	0
13	0.83254	5.780177	Non-mangrove	0	0.3159	0
14	0.827136	5.781802	Non-mangrove	0	0.1888	0
15	0.819716	5.78478	Mangrove	1	0.6365	1
16	0.81909	5.783891	Mangrove	1	0.6637	1
17	0.820588	5.781452	Non-mangrove	0	0.2535	0
18	0.823587	5.782645	Non-mangrove	0	0.1725	0
19	0.82184	5.779952	Non-mangrove	0	0.3587	0
20	0.822392	5.786751	Mangrove	1	0.6196	1
21	0.820137	5.787159	Mangrove	1	0.6503	1
22	0.81885	5.787033	Mangrove	1	0.6577	1
23	0.822173	5.780719	Mangrove	1	0.5601	1
24	0.824265	5.784166	Mangrove	1	0.5919	1
25	0.831918	5.785726	Non-mangrove	0	0.2361	0
26	0.833042	5.782977	Non-mangrove	0	0.1397	0
27	0.821733	5.787165	Mangrove	1	0.6676	1
28	0.820777	5.784488	Mangrove	1	0.6400	1
29	0.826094	5.786577	Non-mangrove	0	0.2370	0
30	0.829475	5.786295	Non-mangrove	0	0.2305	0
31	0.824761	5.780004	Non-mangrove	0	0.3058	0
32	0.819211	5.78447	Mangrove	1	0.6635	1
33	0.819304	5.786516	Mangrove	1	0.5757	1
34	0.823834	5.788001	Mangrove	1	0.6105	1
35	0.823086	5.787044	Mangrove	1	0.6073	1
36	0.832209	5.782419	Non-mangrove	0	0.3106	0
37	0.835205	5.782366	Non-mangrove	0	0.2609	0
38	0.835403	5.780962	Non-mangrove	0	0.2777	0
39	0.830399	5.788276	Non-mangrove	0	0.2120	0
40	0.825916	5.779297	Non-mangrove	0	0.2560	0
41	0.82607	5.78029	Non-mangrove	0	0.2646	0
42	0.827217	5.780787	Non-mangrove	0	0.4239	0
43	0.827865	5.781232	Non-mangrove	0	0.3426	0
44	0.826389	5.779633	Non-mangrove	0	0.3179	0
45	0.824062	5.7804	Non-mangrove	0	0.5771	1
46	0.821676	5.781658	Non-mangrove	0	0.2452	0
47	0.823489	5.78219	Non-mangrove	0	0.1846	0
48	0.820136	5.785864	Non-mangrove	0	0.3118	0
49	0.822284	5.786056	Mangrove	1	0.6308	1
50	0.822198	5.784521	Mangrove	1	0.6495	1

Table 3.6: Table showing ground truth points and CMRI interpretations

			Ground truth		CMRI	
Site	Lon	Lat	Feature	Interpreted value	Value	Interpreted Value
1	0.821402	5.783596	Mangrove	1	0.6557	1
2	0.823438	5.779584	Non-mangrove	0	0.5306	1
3	0.827746	5.77963	Non-mangrove	0	0.2586	0
4	0.830774	5.782509	Non-mangrove	0	0.1772	0
5	0.828359	5.785351	Non-mangrove	0	0.2635	0
6	0.827626	5.784063	Non-mangrove	0	0.2455	0
7	0.828669	5.781467	Non-mangrove	0	0.5701	1
8	0.828435	5.788588	Non-mangrove	0	0.2271	0
9	0.824929	5.787097	Mangrove	1	0.5728	1
10	0.835487	5.784551	Non-mangrove	0	0.1536	0
11	0.835653	5.781888	Non-mangrove	0	0.2351	0
12	0.835118	5.78137	Non-mangrove	0	0.3088	0
13	0.83254	5.780177	Non-mangrove	0	0.3159	0
14	0.827136	5.781802	Non-mangrove	0	0.1888	0
15	0.819716	5.78478	Mangrove	1	0.6365	1
16	0.81909	5.783891	Mangrove	1	0.6637	1
17	0.820588	5.781452	Non-mangrove	0	0.2535	0
18	0.823587	5.782645	Non-mangrove	0	0.1725	0
19	0.82184	5.779952	Non-mangrove	0	0.3587	0
20	0.822392	5.786751	Mangrove	1	0.6196	1
21	0.820137	5.787159	Mangrove	1	0.6503	1
22	0.81885	5.787033	Mangrove	1	0.6577	1
23	0.822173	5.780719	Mangrove	1	0.5601	1
24	0.824265	5.784166	Mangrove	1	0.5919	1
25	0.831918	5.785726	Non-mangrove	0	0.2361	0
26	0.833042	5.782977	Non-mangrove	0	0.1397	0
27	0.821733	5.787165	Mangrove	1	0.6676	1
28	0.820777	5.784488	Mangrove	1	0.6400	1
29	0.826094	5.786577	Non-mangrove	0	0.2370	0
30	0.829475	5.786295	Non-mangrove	0	0.2305	0
31	0.824761	5.780004	Non-mangrove	0	0.3058	0
32	0.819211	5.78447	Mangrove	1	0.6635	1
33	0.819304	5.786516	Mangrove	1	0.5757	1
34	0.823834	5.788001	Mangrove	1	0.6105	1
35	0.823086	5.787044	Mangrove	1	0.6073	1
36	0.832209	5.782419	Non-mangrove	0	0.3106	0
37	0.835205	5.782366	Non-mangrove	0	0.2609	0
38	0.835403	5.780962	Non-mangrove	0	0.2777	0
39	0.830399	5.788276	Non-mangrove	0	0.2120	0
40	0.825916	5.779297	Non-mangrove	0	0.2560	0

41	0.82607	5.78029	Non-mangrove	0	0.2646	0
42	0.827217	5.780787	Non-mangrove	0	0.4239	0
43	0.827865	5.781232	Non-mangrove	0	0.3426	0
44	0.826389	5.779633	Non-mangrove	0	0.3179	0
45	0.824062	5.7804	Non-mangrove	0	0.5771	1
46	0.821676	5.781658	Non-mangrove	0	0.2452	0
47	0.823489	5.78219	Non-mangrove	0	0.1846	0
48	0.820136	5.785864	Non-mangrove	0	0.3118	0
49	0.822284	5.786056	Mangrove	1	0.6308	1
50	0.822198	5.784521	Mangrove	1	0.6495	1

Table 3.7 Table showing ground truth points and supervised classification interpretations

			Ground truth		Supervised	
Site	Lon	Lat	Feature	Interpreted value	Value	Interpreted Value
1	0.821402	5.783596	Mangrove	1	2	1
2	0.823438	5.779584	Non-mangrove	0	6	0
3	0.827746	5.77963	Non-mangrove	0	8	0
4	0.830774	5.782509	Non-mangrove	0	5	0
5	0.828359	5.785351	Non-mangrove	0	6	0
6	0.827626	5.784063	Non-mangrove	0	7	0
7	0.828669	5.781467	Non-mangrove	0	6	0
8	0.828435	5.788588	Non-mangrove	0	6	0
9	0.824929	5.787097	Mangrove	1	2	1
10	0.835487	5.784551	Non-mangrove	0	5	0
11	0.835653	5.781888	Non-mangrove	0	6	0
12	0.835118	5.78137	Non-mangrove	0	6	0
13	0.83254	5.780177	Non-mangrove	0	5	0
14	0.827136	5.781802	Non-mangrove	0	5	0
15	0.819716	5.78478	Mangrove	1	2	1
16	0.81909	5.783891	Mangrove	1	2	1
17	0.820588	5.781452	Non-mangrove	0	1	0
18	0.823587	5.782645	Non-mangrove	0	1	0
19	0.82184	5.779952	Non-mangrove	0	5	0
20	0.822392	5.786751	Mangrove	1	2	1
21	0.820137	5.787159	Mangrove	1	2	1
22	0.81885	5.787033	Mangrove	1	2	1
23	0.822173	5.780719	Mangrove	1	2	1
24	0.824265	5.784166	Mangrove	1	2	1
25	0.831918	5.785726	Non-mangrove	0	5	0

26	0.833042	5.782977	Non-mangrove	0	1	0
27	0.821733	5.787165	Mangrove	1	2	1
28	0.820777	5.784488	Mangrove	1	2	1
29	0.826094	5.786577	Non-mangrove	0	5	0
30	0.829475	5.786295	Non-mangrove	0	6	0
31	0.824761	5.780004	Non-mangrove	0	6	0
32	0.819211	5.78447	Mangrove	1	2	1
33	0.819304	5.786516	Mangrove	1	2	1
34	0.823834	5.788001	Mangrove	1	2	1
35	0.823086	5.787044	Mangrove	1	2	1
36	0.832209	5.782419	Non-mangrove	0	5	0
37	0.835205	5.782366	Non-mangrove	0	6	0
38	0.835403	5.780962	Non-mangrove	0	6	0
39	0.830399	5.788276	Non-mangrove	0	5	0
40	0.825916	5.779297	Non-mangrove	0	6	0
41	0.82607	5.78029	Non-mangrove	0	6	0
42	0.827217	5.780787	Non-mangrove	0	6	0
43	0.827865	5.781232	Non-mangrove	0	6	0
44	0.826389	5.779633	Non-mangrove	0	6	0
45	0.824062	5.7804	Non-mangrove	0	3	0
46	0.821676	5.781658	Non-mangrove	0	1	0
47	0.823489	5.78219	Non-mangrove	0	1	0
48	0.820136	5.785864	Non-mangrove	0	1	0
49	0.822284	5.786056	Mangrove	1	2	1
50	0.822198	5.784521	Mangrove	1	2	1

To assess the performance of the various techniques of mapping out mangroves in the study area, a UAV imagery of very high resolution was used. The UAV imagery however covered a smaller part of the study area, 1.88 km^2 of the study area and therefore the various resultant classifications, that is the NDVI, CMRI and the supervised were clipped to the size of the UAV imagery for further analysis. A visual analysis was first carried out, a simple method of comparison (Mohammady, Moradi, Zeinivand, & Temme, 2015), where the three resulting maps were overlaid on the UAV imagery to clearly see how well each technique was able to cover the mangrove area is shown in Figure 3.9.

As mentioned earlier, the UAV imagery was used as the validation data due to its high resolution. However, the bands of the UAV available were RGB and thus a more uniform

means of validation was required. This resulted in the use of the binary form of data as shown in Table 3.5, 3.6 and 3.7. As mentioned earlier, 50 random points were selected on the UAV imagery. Areas of mangroves that coincided with mangrove areas were coded as “1”, non-mangrove as “0”. These 50 points were overlaid on each clipped map and the corresponding values and interpreted values extracted, again this can be seen in Table 3.5 (NDVI), Table 3.6 (CMRI) and Table 3.7 (supervised) after which the Cochran’s Q test was used to derive the P-value for each technique used using the UAV imagery as the standard.

The area coverage of mangroves from each technique was then calculated. Python scripting was used to generate the area coverage of mangroves in the semi-automatic mapped images whiles that of the supervised classification was calculated by multiplying the sum of count of the mangrove class by the area on one pixel.

Figure 3. 9: UAV imagery overlaid on NDVI map

CHAPTER FOUR

RESULTS

4.1 Normalized Difference Vegetation Index (NDVI)

The resulting map after the NDVI classification as shown in Figure 4.1 was derived from the NIR and the Red band. NDVI values range from -1 to +1 with areas of water having values close to -1 whiles areas of bare land, rocks and buildings with values closer to +1. Areas with vegetation were observed to have high NDVI values of between 0.27 and 0.37, as shown in Figure 4.1. From the map, two different colours depicted the area covered by water which could be as a result of the difference in salinity of the lagoon at different parts. The observed NDVI vegetation values were used to set thresholds to exclusively map out areas of vegetation including mangroves and was used to generate a colour maps as observed in figure 4.2.

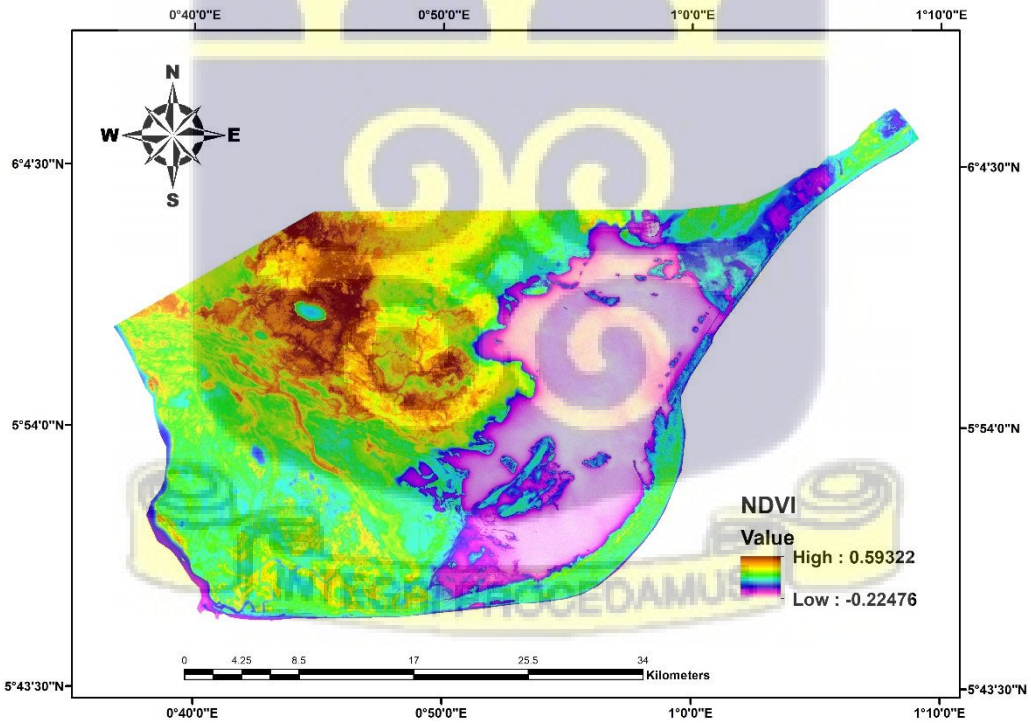

Figure 4. 1: NDVI classification of study area

From the threshold map, it was observed that there were some patches of other vegetation with similar NDVI values as that of mangroves. Using the threshold values of mangroves ranging between 0.27 and 0.35, the area covered by mangroves was estimated to be 23.4%. Areas of other vegetation and other features including built-up and bare soil were within NDVI values of 0.35 to 0.59. Areas with water bodies were within NDVI values of between -0.22 to 0.27.

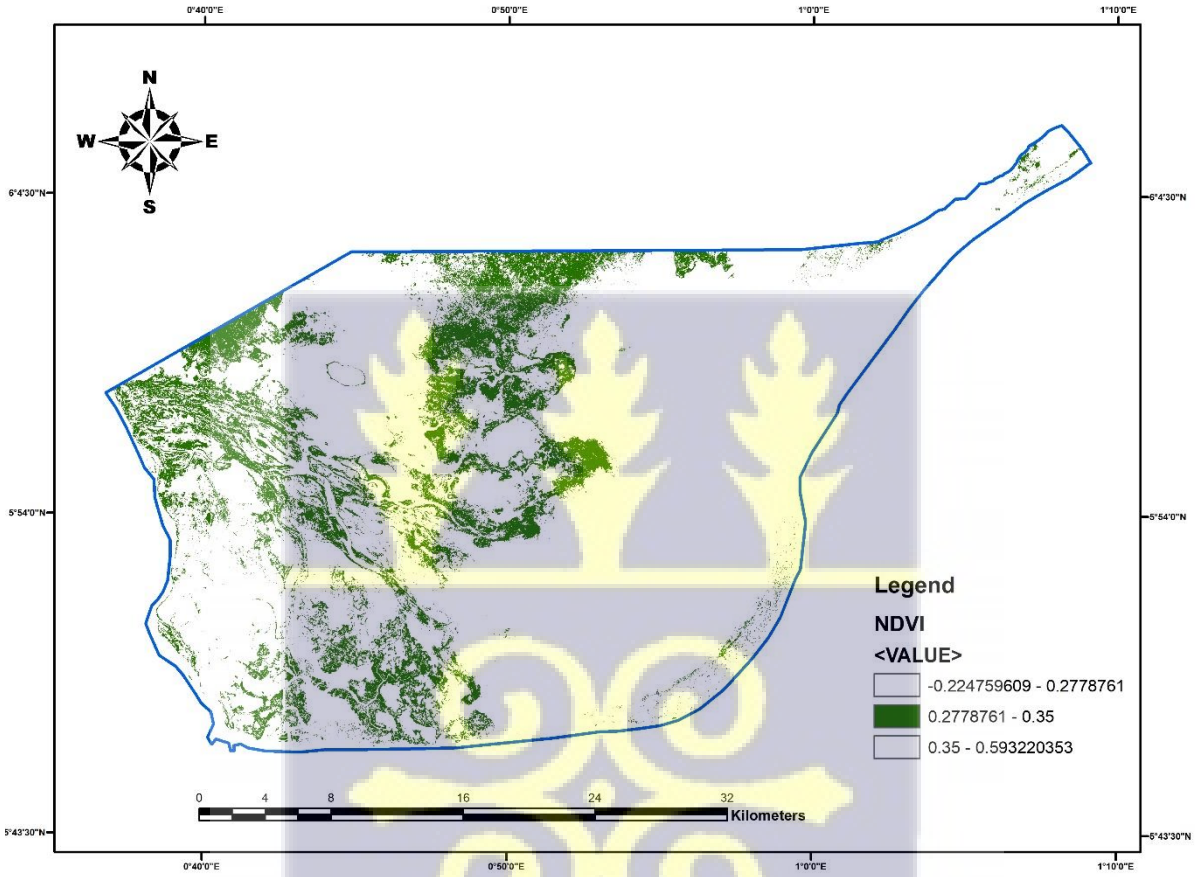

Figure 4. 2: NDVI map showing mangrove threshold between 0.27 and 0.35

4.2 Combined Mangrove Recognition Index (CMRI)

To generate a CMRI map, the formula used included subtracting NDWI values from NVDI values at pixel level(Gupta et al., 2018). Higher values of NDVI indicate sufficient moisture and that was observed in the NDWI map in Figure 4.3. Moisture content of features were observed to have NDWI values of 0.24 and -0.50 with areas of water bodies recording the highest.

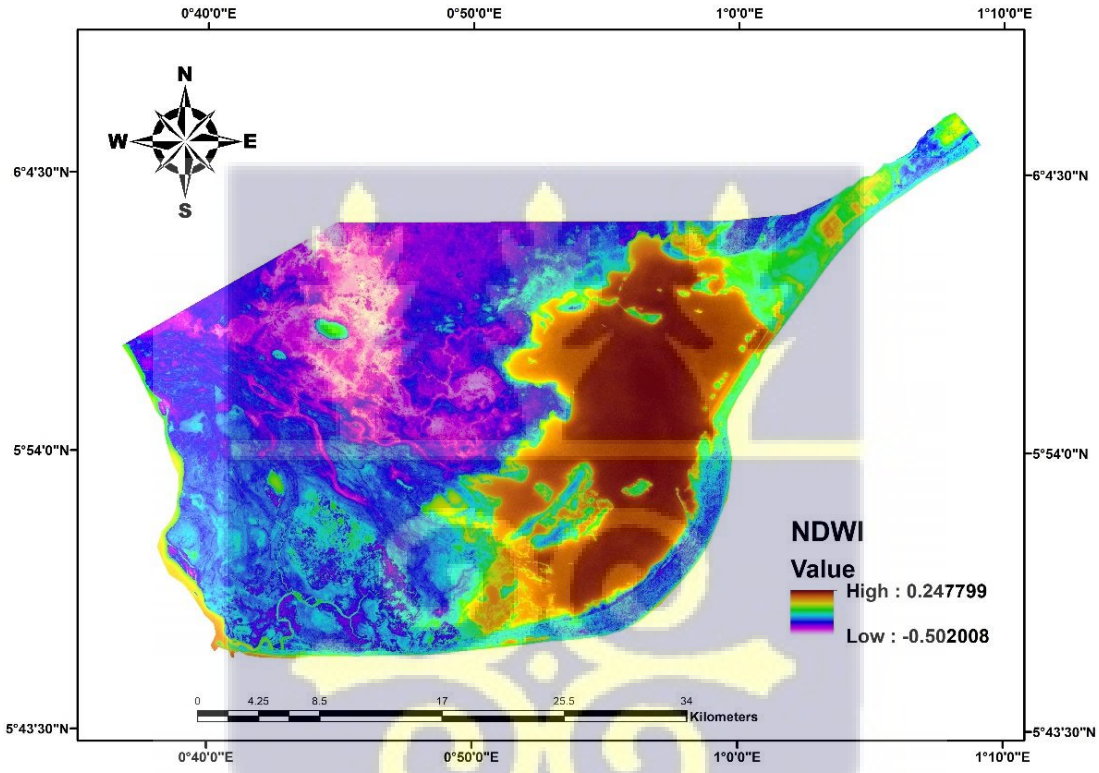

Figure 4. 3: NDWI classification of study area

Figure 4.4 shows CMRI map with mangrove areas observed to have values ranging between 0.51 and 0.70. Areas with water bodies were observed to have very low CMRI values with the lowest of -0.42. However, areas with other vegetation were observed to have positive CMRI values.

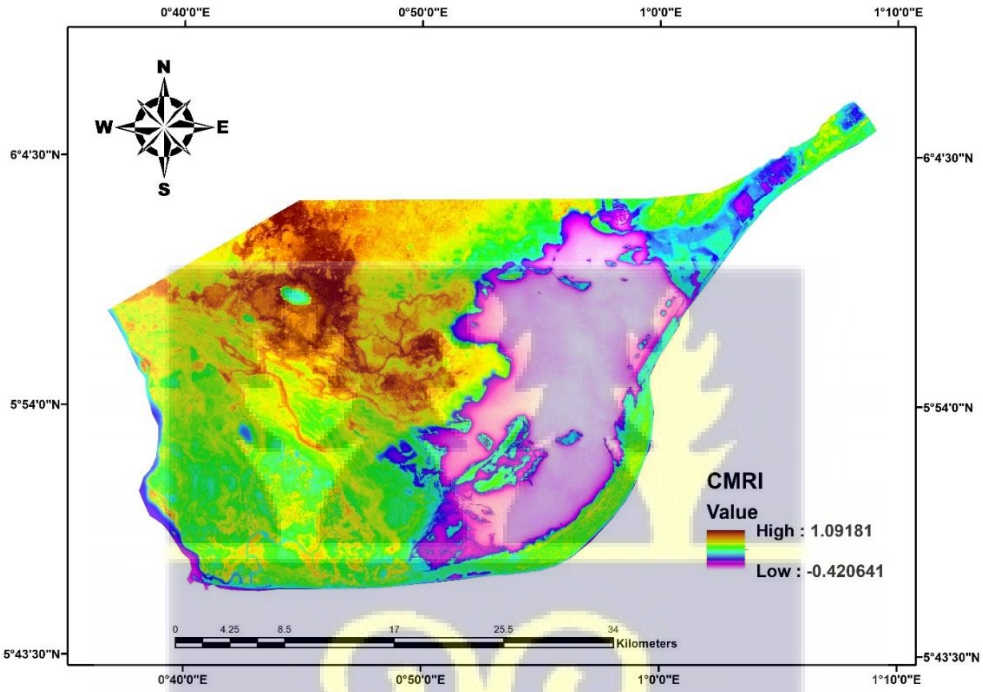

Figure 4. 4: CMRI classification of study area

As seen in the threshold map, Figure 4.5, areas of mangroves are clearly mapped out with large areas of water falling with the range 0.7 and 1.0. Areas with other vegetation were observed to fall within the range of 0.4 and 0.5. Using the threshold values of 0.5 and 0.7 which is observed for mangrove vegetation, the area estimated for mangrove area coverage was 24.02%.

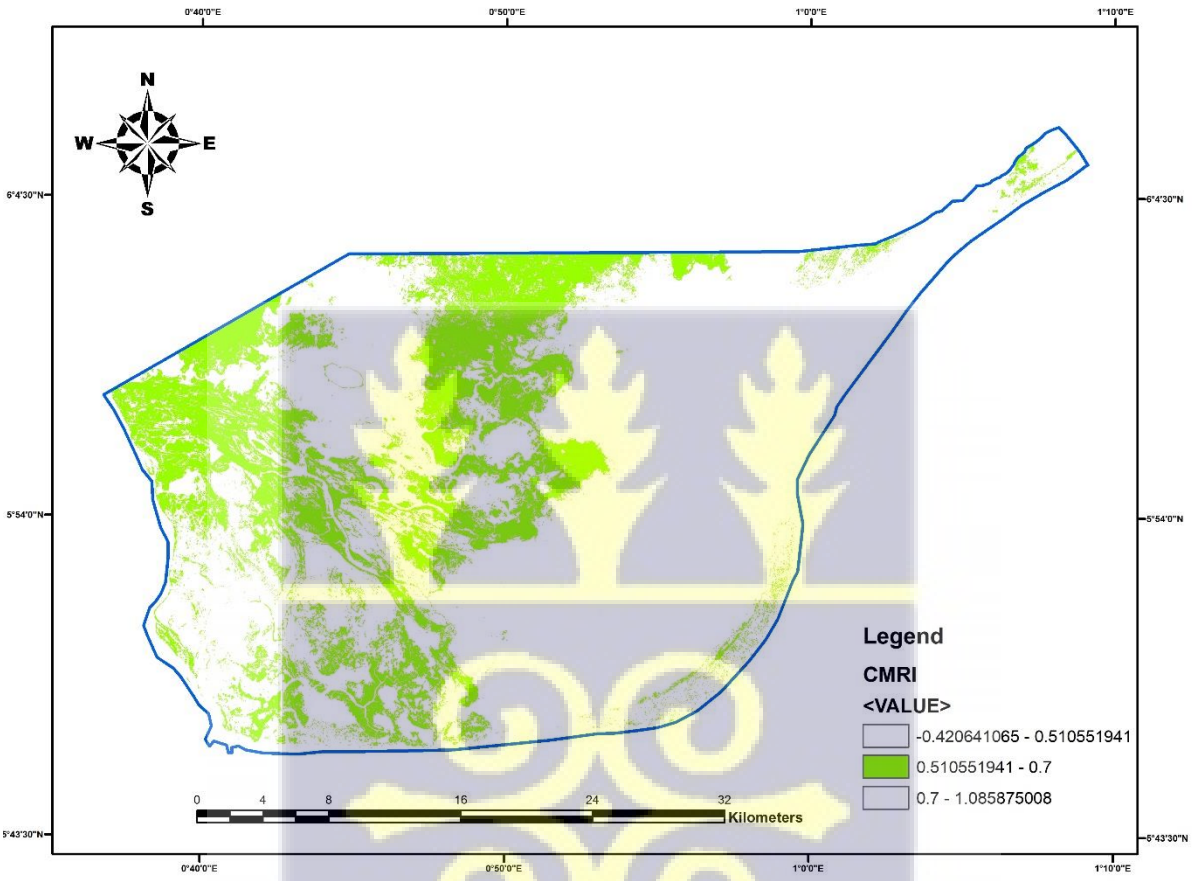

Figure 4. 5: CMRI threshold map showing mangroves between the values of 0.5 and 0.7

4.3 Supervised Classification

The Maximum Likelihood Classification (MLC) was used to carry out the classification of eight (8) classes or features. The classes include water, mangrove, other vegetation, natural beach, mudflat, built-up, saltpan and bare ground (Table 3.4). The resulting map can be observed in Figure 4.6. Areas with water bodies were clearly mapped out with a dark blue colour. Areas of mangroves were also mapped out with dark green with other vegetation with the lighter shade of green. There were some areas of mudflats which were mapped out as built-up in the final output as a result of similar reflectance. Generally, the mapping of mangroves was fairly accurate when visually observed when compared to other vegetation as can be clearly observed in Figure 4.6.

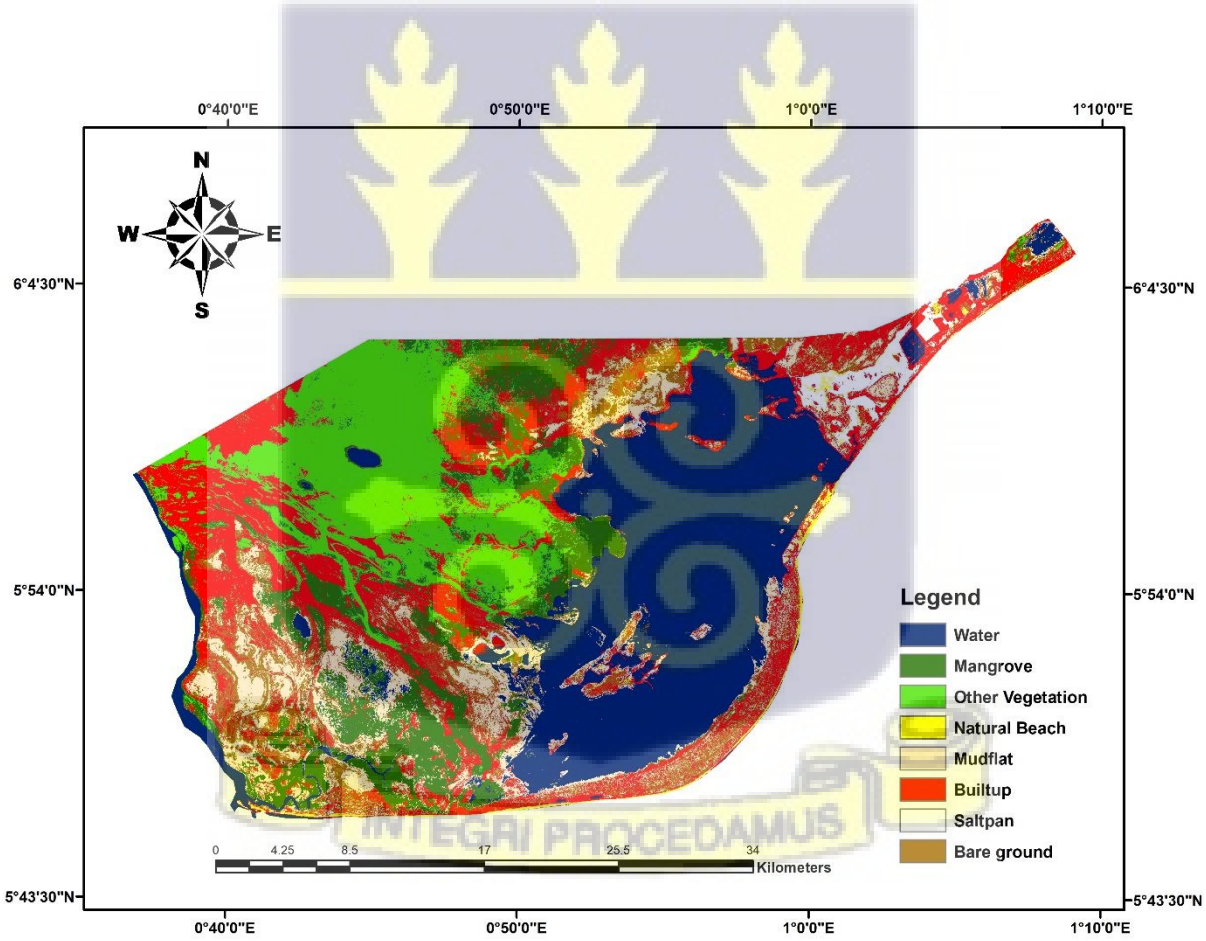

Figure 4. 6: Supervised classification map showing various classes

4.4 Performance and Validation

The performance of the NDVI, CMRI and the supervised technique of mapping out of mangroves was done visually and by the area of mangrove extent. Figure 4.7 shows the mangroves mapped out; supervised (a), CMRI (b), NDVI (c) and the reference UAV image, (c). It was observed that the CMRI mapped out an area of 0.25 km^2 of mangroves, followed by the supervised and NDVI, 0.30 km^2 and 0.32 km^2 respectively, Figure 4.8. The Cochran's Q test carried out for the P-value of NDVI and the CMRI using the UAV imagery as the reference image resulted in both NDVI and CMRI with P-values of P>0.05 which in effect means that there is no significant difference in areas of mangroves mapped out by both indices.

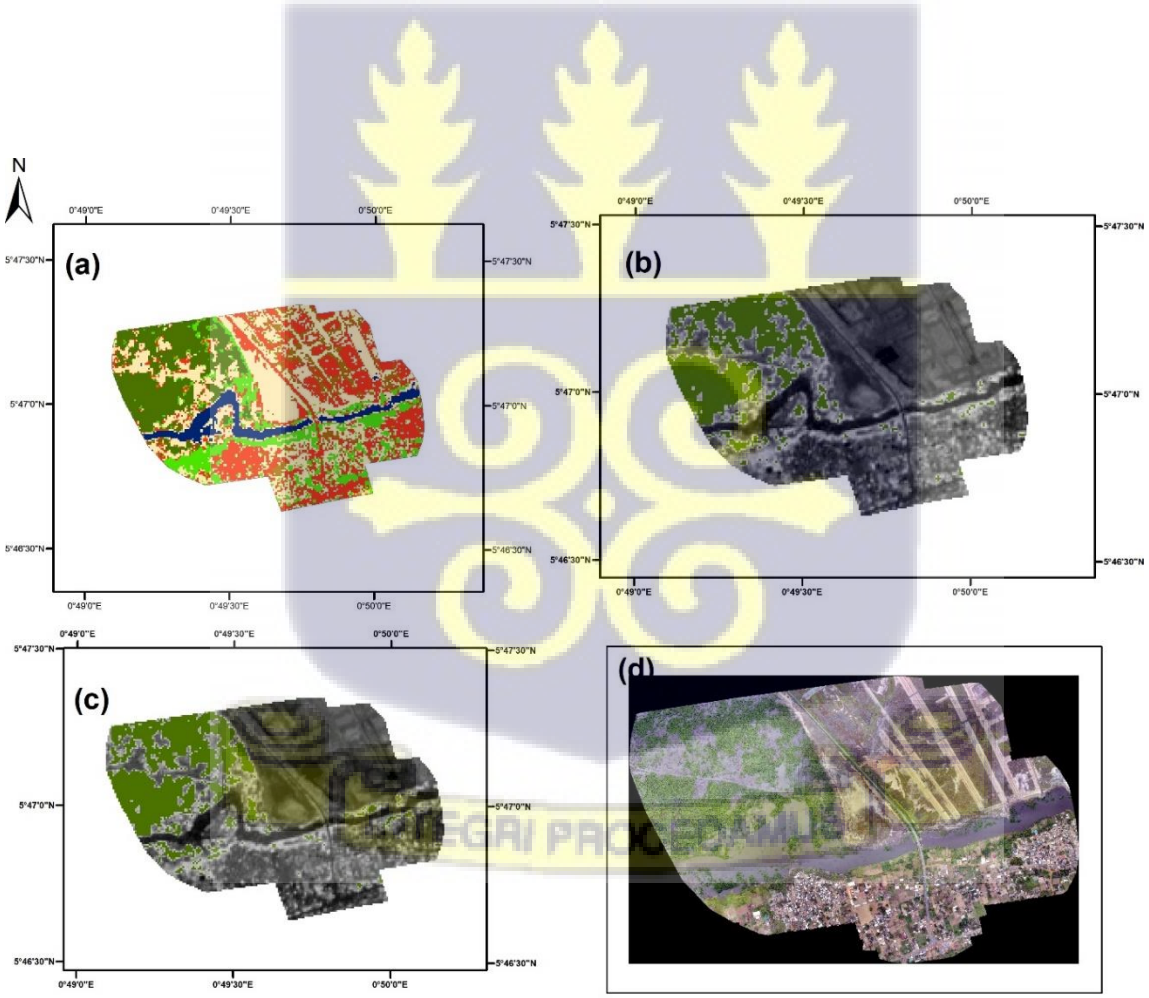

Figure 4. 7: Supervised (a), CMRI (b), NDVI (c) classification techniques showing mangrove areas in green. UAV imagery (d) of subset area used for validation

The area mapped out when the imagery was clipped to the size of UAV imagery can be observed in Table 4.1. Area of mangroves were estimated to be 13.32% for CMRI, 16.19% for maximum-likelihood, and 17.16% for NDVI. The area of mangroves estimated from the UAV imagery was 12.96%.

Table 4.1 Table showing the area mapped out by each technique and the UAV imagery

Technique	Area (%)
NDVI	17.16
Supervised	16.19
CMRI	13.32
UAV	12.96

Figure 4.8 shows the area of mangrove estimated in square kilometres. The total area covered by the imagery was 1.88 km^2. The area of mangroves was estimated to be 0.30 km^2 for maximum-likelihood, 0.32 km^2 for NDVI and 0.25 km^2 for CMRI. From the UAV imagery, the area covered by mangroves was 0.24 km^2.

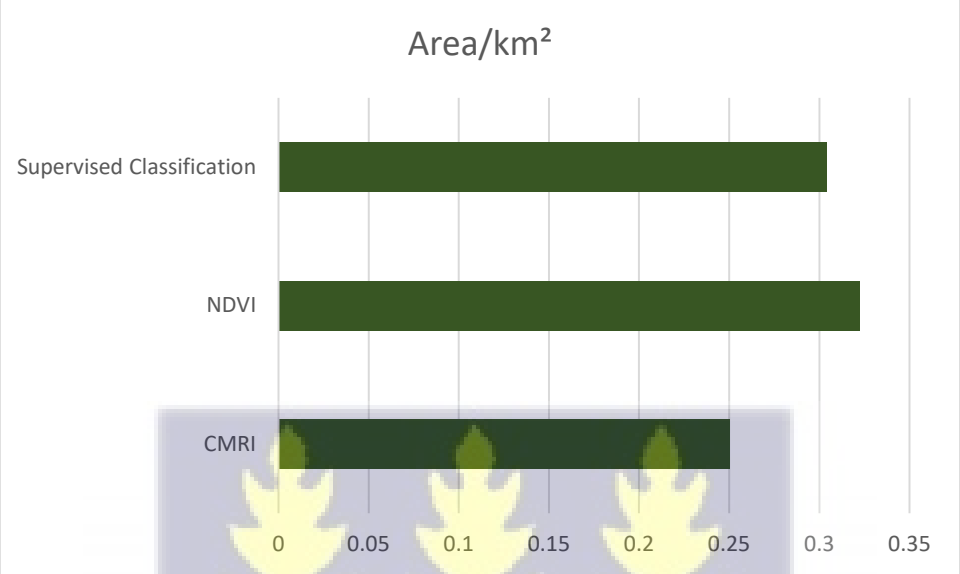

Figure 4. 8: Mangrove area coverage of the three classification techniques

CHAPTER FIVE

DISCUSSION

5.1 Mangrove Mapping

Mangrove forests play a very important role in the coastal ecosystem because of their strategic locations. They serve as a natural protection for the coast; the aerial roots of mangroves retain sediments preventing the coastline from erosion. The roots also help form a natural barrier against violent storm surges, oncoming waves and also reduces risks from flooding. Mangroves serve as a safe haven for endangered species and also serve as breeding places for many organisms. They serve as a source of fish, fuelwood and wood for medicine, construction and the tanning of fish by local communities. Carbon sequestration by mangroves make them very important in recent times as more awareness have been put on climate change. There serve as a natural means of reducing the carbon in the atmosphere.

Due to the increase in population in the coastal zone globally, mangrove forests are threatened. The mangrove ecosystem is largely being destroyed for other land use such as urban development, farming, just to mention few which have detrimental effects on the coastal ecosystem at large. It is however important that the ecosystem is protected and thus monitoring of their status globally is important for effective management (Friess et al., 2019). The nature of mangrove ecosystem makes it difficult for field surveys to be carried out regular, however, the use of Earth Observation (EO) data, which in this study the optical sensor of the Sentinel-2 was used has made it easier for researchers to carryout studies by taking advantage of remote sensing technology and techniques. The use of satellites makes it possible to map out wide areas of vegetation effectively. The most widely used means of monitoring vegetation is the use of vegetation indices making use of the spectral response of vegetation to detect and estimate the extent of coverage (Xie et al., 2008).

The Keta Lagoon Complex, an area with the abundance of mangrove stands was classified using the NDVI, CMRI and the supervised classification techniques. The NDVI is the most widely used vegetation estimating technique (Taufik, Syed Ahmad, & Azmi, 2019). In this study, the CMRI index developed by Gupta et. al (2018), for mapping out mangroves was used in mapping out mangroves in Keta Lagoon complex and was compared to NDVI and supervised classification. The classification algorithm used for the supervised classification was the MLC.

Supervised classification technique is usually used when the researcher has prior knowledge about the area of classification (Yiqiang et al. 2010). The location in this study is however a known and a visited area, UAV imagery of a sub-area within the Keta Lagoon complex, Salo, a suburb within the lagoon catchment was used for validation and testing of performance of the various indices used. Using the supervised classification was very time consuming because enough training samples needed to be carefully selected to reduce spectral mixing to the minimum and ensure a high level of classification accuracy. Unlike the supervised classification, the application of the NDVI and CMRI was less time-consuming. Once the formula is applied, the software automatically classifies the imagery and produces resulting NDVI and CMRI values which indicate various classification features. NDVI values of vegetation in this study were observed to be between 0.27 and 0.37 which are less than the expected values for dense vegetations, values above 0.4, and values between 0.2 and 0.4 represent areas of sparse vegetation (Mohammady et al. 2015; J. Wang et al. 2005). In the study by Mohammad et al., (2015), areas of NDVI values of 0.6 and above were classified as areas of dense forests, it was however suggested that the combination of both supervised and unsupervised classifications produce better accuracy. The reason for the low NDVI value recorded in this study may be attributed to the season in which the imagery was taken, in this case the harmattan period characterised by dusty winds and dryness. Harmattan occurs within

the period of November and the middle of March and within this period, most vegetation lose moisture content in their leaves due to drought (Burton et al., 2013). This may have affected the results obtained for the NDVI values for other vegetation and mangroves. The other values however conformed to expected values, areas where water bodies were located showed values close to -1 whiles areas of bare land, rocks and buildings produced values between the range of -0.1 and 0.1. CMRI values observed for mangroves were between 0.51 and 0.70.

5.2 Performance of Indices and Supervised Classification

The performance of the semi-automatic indices and the supervised classification methods were based on area coverage basis and visualization using UAV imagery as the validation data. The area coverage of vegetation generally in NDVI was observed to be 0.32 km^2. This was due to the nature of the NDVI mapping out all areas of green vegetation which included mangrove areas. The area coverage of mangroves from CMRI was 0.25 km^2 as against 0.30 km^2 of that of supervised classification technique. This also reveals that the CMRI index is more sensitive to the mangroves and hence was able to map them out with a higher accuracy. It was observed that in the supervised classification using the MLC algorithm, there was the instance of pixel mixing due to the similarity in spectral reflectance of other vegetation and that of mangroves despite including many training samples also observed by Mohammady et al. (2015). According to Rozenstein and Karnieli (2010), in areas where there are a large number of green vegetation, using the selection of areas as training samples is difficult and thus suggest that the unsupervised technique be used after which the resulting data may be fine-tuned. The p-value recorded when the various indices were tested against the UAV imagery resulted in 0.08 for NDVI, 0.08 for CMRI and 0.06 for supervised classification. These values are >0.05 and thus can be interpreted to mean no significant difference exists between the various techniques used

and the validation imagery, which means all the techniques used were able to effectively map out areas of mangroves in this study.

CHAPTER SIX

CONCLUSION

6.1 Conclusion

This study confirms the ability of CMRI in the mapping of mangroves. A study by Gupta et al (2018) made use of the Landsat 8 OLI mission where the Green, Red and NIR with the range of wavelengths of bands 0.533–0.590, 0.64–0.67 and 0.85–0.87 (Green, Red and NIR respectively) were used to generate the index. This study was carried out using the Sentinel-2A sensor to generate the index making use of the Green, Red and NIR with wavelengths of 0.560, 0.665 and 0.842 (Green, Red and NIR respectively) also available in other optical sensors with multiple bands. It has been confirmed that this index can be applied on satellite images from other sensors and can perform accurately as observed in this study where mangroves in the Keta Lagoon Complex were mapped out effectively from other vegetation as compared to the NDVI which is also a semi-automatic classification technique and the supervised classification using MLC algorithm. The CMRI values of mangroves were found to be between 0.51 and 0.70 which was used to clearly delineate mangroves from other classes making it easy for the pixel values of mangroves areas to be extracted and calculated. This study used python scripting for the extraction of both NDVI and CMRI values which took less time as compared to when using a software for area analysis as was carried out with that of the supervised classification.

6.2 Recommendation

It is recommended that further studies to detect mangroves should be carried out using SAR data or a combination with optical data to improve the prediction accuracy to better enhance the sensitivity of the index. It is also recommended that the process of mapping out mangroves be automated to allow for a large volume of data set to analysed in minimum time to enhance continuous monitoring of this important coastal ecosystem. Again, studies on discriminating mangrove at the species level should be carried out for better management conservation of mangrove forest.

REFERENCES

Ajonina, G., Diamé, A., & Kairo, J. (2018). Current status and conservation of mangroves in Africa: An overview. *Journal of Chemical Information and Modeling*, *53*(9), 1689–1699.

Alonso, A., Muñoz-Carpena, R., Kennedy, R. E., & Murcia, C. (2016). Wetland landscape spatio-temporal degradation dynamics using the new google earth engine cloud-based platform: Opportunities for non-specialists in remote sensing. Transactions of the American Society of Agricultural and Biological Engineers (ASABE), 59(5), 1333–1344. https://doi.org/10.13031/trans.59.11608

Armah. Kojo Ayaa; Diame, Abdoulaye; Ajonina, Gordon; Kairo, J. (2009). The role and work of African Mangrove Network (AMN) in conservation and sustainable use of mangroves in Africa. Nature & Faune, 30–41. Retrieved from http://www.fao.org/3/a-ak995e/ak995e02.pdf

Arun Prasad, K., & Gnanappazham, L. (2014). Species Discrimination of Mangroves using Derivative Spectral Analysis. ISPRS Annals of Photogrammetry, Remote Sensing and Spatial Information Sciences, II–8(December), 45–52. https://doi.org/10.5194/isprsannals-ii-8-45-2014

Burton, R. R., Devine, G. M., Parker, D. J., Chazette, P., Dixon, N., Flamant, C., & Haywood, J. M. (2013). The harmattan over West Africa: Nocturnal structure and frontogenesis. Quarterly Journal of the Royal Meteorological Society, 139(674), 1364–1373. https://doi.org/10.1002/qj.2036

Center, C. R. (2013). Managing our coastal wetlands: Lessons from the Western Region.USAID Integrated Coastal and Fisheries Governance Program for the Western Region of Ghana. (January), 4.

Carrere, R. (2002). Mangroves: Local Livelihoods vs. Corporate Profits. World Rainforest Movement.

Central Intelligence Agency (2006). CIA World Factbook. Available at https://www.cia.gov/cia/publications/fact book/index.html (accessed 3 July 2006).

Chape, S., Harrison, J., Spalding, M. and Lysenko, I. (2005). Measuring the extent and effectiveness of protected areas as an indicator for meeting global biodiversity targets. Philosophical Transactions of the Royal Society B: Biological Sciences 360 (1454): 443–455

Coastal Resources Center and Friends of the Nation. (2011). Assessment of Critical Coastal Habitats of the Western Region, Ghana. Integrated Coastal and Fisheries Governance Initiative for the Western Region of Ghana., 132.

Cochran, W. G. (1954). Some methods for strengthening the common chi-square tests.

Biometrics, 10, 417–451.

Corcoran, E., Ravilious, C. and Skuja, M., (2007.). Mangroves of Western and Central Africa Report produced for UNEP-DEPI under the UNEP Biodiversity Retated Projects in Africa. Retrieved from http://www.archive.org/details/mangrovesofweste07corc

Dayton, P., Kaufman, M. M., Marsh, W. M., & Kaufman, M. M. (2012). Coastal Systems. Ecosystems and Human Well-Being: Current State and Trends, 513–549. https://doi.org/10.1017/cbo9781139019507.023

Friess, D. A., Rogers, K., Lovelock, C. E., Krauss, K. W., Hamilton, S. E., Lee, S. Y., Shi, S. (2019). The State of the World's Mangrove Forests: Past, Present, and Future. Annual Review of Environment and Resources, 44(1), 89–115. https://doi.org/10.1146/annurev-environ-101718-033302

Ghosh, M. K., Kumar, L., & Roy, C. (2016). Mapping long-term changes in mangrove species composition and distribution in the Sundarbans. Forests, 7(12). https://doi.org/10.3390/f7120305

Giri, C. (2016). Observation and monitoring of mangrove forests using remote sensing: Opportunities and challenges. Remote Sensing, 8(9). https://doi.org/10.3390/rs8090783

Gupta, K., Mukhopadhyay, A., Giri, S., Chanda, A., Datta Majumdar, S., Samanta, S., Hazra, S. (2018). An index for discrimination of mangroves from non-mangroves using LANDSAT 8 OLI imagery. MethodsX, 5(September), 1129–1139. https://doi.org/10.1016/j.mex.2018.09.011

Henry, M. J. (2016). Climate Change and Blue Carbon: Above-Ground Carbon Stock of Mangroves in the Lower Volta Area. University of Ghana, Legon.

Heumann, B. W. (2011a). An object-based classification of mangroves using a hybrid decision tree-support vector machine approach. Remote Sensing, 3(11), 2440–2460. https://doi.org/10.3390/rs3112440

Heumann, B. W. (2011b). Satellite remote sensing of mangrove forests: Recent advances and future opportunities. Progress in Physical Geography, 35(1), 87–108. https://doi.org/10.1177/0309133310385371

Huang, X., Zhang, L., & Wang, L. (2009). Evaluation of Morphological Texture Features for Mangrove Forest Mapping and Species Discrimination Using Multispectral IKONOS Imagery. IEEE Geoscience and Remote Sensing Letters, 6(3), 393–397.

Joshi, H., & Ghose, M. (2003). Forest structure and species distribution along soil salinity and pH gradient in mangrove swamps of the Sundarbans. Tropical Ecology, 44(2), 197–206.

Kathiresan, K., & Bingham, B. L. (2001). Biology of mangroves and mangrove ecosystems. Advances in Marine BiologyKathiresan, K., & Bingham, B. L. (2001). Biology of Mangroves and Mangrove Ecosystems. Advances in Marine Biology, 40, 81–251. Https://Doi.Org/10.1016/S0065-2881(01)40003-4, 40, 81–251. https://doi.org/10.1016/S0065-2881(01)40003-4

Ke, Y., Quackenbush, L. J., & Im, J. (2010). Synergistic use of QuickBird multispectral imagery and LIDAR data for object-based forest species classification. Remote Sensing of Environment, 114(6), 1141–1154. https://doi.org/10.1016/j.rse.2010.01.002

Kuenzer, C., Bluemel, A., Gebhardt, S., Quoc, T. V., & Dech, S. (2011). Remote sensing of mangrove ecosystems: A review. In Remote Sensing (Vol. 3). https://doi.org/10.3390/rs3050878

Lamptey, A.M.; Ofori-Danson, P.K.; Abbenney-Mickson, S.; Breuning-Madsen, H.; Abekoe, M.K. (2013). The Influence of Land-Use on Water Quality in a Tropical Coastal Area: Case Study of the Keta Lagoon Complex, Ghana, West Africa. Open J. Mod. Hydrol., 3, 188–195.

Lamptey, E.; Armah, A.K. (2008). Factors Affecting Macrobenthic Fauna in a Tropical Hypersaline Coastal Lagoon in Ghana, West Africa. Estuaries Coasts 2008, 31, 1006–1019.

Medeiros, T. C. C., Sampaio, E., & Nascimento, D. M. (2018). Leaf area index and vegetation cover of the Paripe river mangrove, Pernambuco, Brazil, in 1997 and 2017. Journal of Integrated Coastal Zone Management, 18(1), 41–48. https://doi.org/10.5894/rgci-n119

Mensah, J. (2013). Remote Sensing Application for Mangrove Mapping in the Ellembelle District in Ghana. Retrieved from http://fonghana.org/wp-content/uploads/2014/01/REMOTE-SENSING-APPLICATION-FOR-MANGROVE-MAPPING-IN-THE-ELLEMBELLE-DISTRICT-IN-GHANA.pdf

Mohammady, M., Moradi, H. R., Zeinivand, H., & Temme, A. J. A. M. (2015). A comparison of supervised, unsupervised and synthetic land use classification methods in the north of Iran. International Journal of Environmental Science and Technology, 12(5), 1515–1526. https://doi.org/10.1007/s13762-014-0728-3

Myint, S. W., Giri, C. P., Wang, L., Zhu, Z., & Gillete, S. C. (2008). Identifying mangrove species and their surrounding land use and land cover classes using object-oriented approach with a lacunarity spatial measure. GIScience and Remote Sensing, 45(2), 188–208. https://doi.org/10.2747/1548-1603.45.2.188

Navarro, J. A., Algeet, N., Fernández-Landa, A., Esteban, J., Rodríguez-Noriega, P., & Guillén-Climent, M. L. (2019). Integration of UAV, Sentinel-1, and Sentinel-2 data for mangrove plantation aboveground biomass monitoring in Senegal. Remote Sensing, 11(1), 1–23. https://doi.org/10.3390/rs11010077

Nortey, D. D. N., Aheto, D. W., Blay, J., Jonah, F. E., & Asare, N. K. (2016). Comparative Assessment of Mangrove Biomass and Fish Assemblages in an Urban and Rural Mangrove Wetlands in Ghana. Wetlands, 36(4), 717–730. https://doi.org/10.1007/s13157-016-0783-2

Pastor-Guzman, J., Dash, J., & Atkinson, P. M. (2018). Remote sensing of mangrove forest phenology and its environmental drivers. Remote Sensing of Environment, 205(January), 71–84. https://doi.org/10.1016/j.rse.2017.11.009

Pham, T. D., Yokoya, N., Bui, D. T., Yoshino, K., & Friess, D. A. (2019). Remote sensing approaches for monitoring mangrove species, structure, and biomass: Opportunities and challenges. Remote Sensing, 11(3). https://doi.org/10.3390/rs11030230

Polidoro, B. A., Carpenter, K. E., Collins, L., Duke, N. C., Ellison, A. M., Ellison, J. C., Yong, J. W. H. (2010). The loss of species: Mangrove extinction risk and geographic areas of global concern. PLoS ONE, 5(4). https://doi.org/10.1371/journal.pone.0010095

Roslani, M. A., Mustapha, M. A., Lihan, T., & Juliana, W. A. W. (2015). Classification of mangroves vegetation species using texture analysis on Rapideye satellite imagery Classification of Mangroves Vegetation Species Using Texture Analysis on RapidEye Satellite Imagery. 480(December 2013). https://doi.org/10.1063/1.4858701

Sackey, I., Kpikpi, W. M., & Imoro, A. W. M. (2011). Ecological studies in the Iture estuary mangrove forest in Ghana. Journal of the Ghana Science Association, 13(2), 37–44. Retrieved from http://www.ajol.info/index.php/jgsa/article/view/74880

Sheskin, D. J. (2003). Parametric and non-parametric statistical procedures: Third edition. Handbook of Parametric and Nonparametric Statistical Procedures: Third Edition, 1–1193.

Sørensen, T.H.; Vølund, G.; Armah, A.K.; Christiansen, C.; Jensen, L.B.; Pedersen, J.T. (2003) Temporal and Spatial Varations in Concentrations of Sediment Nutrients and Carbon in the Keta Lagoon, Ghana. West. Afr. J. Appl. Ecol., 4, 91–105.

Taufik, A., Syed Ahmad, S. S., & Azmi, E. F. (2019). Classification of landsat 8 satellite data using unsupervised methods. Lecture Notes in Networks and Systems, 67(August 2017), 275–284. https://doi.org/10.1007/978-981-13-6031-2_46

Tyler, J. D., Tyler, J. D., Scott, C. M., & Scott, C. M. (1982). Status and distribution of mangrove forests of the world using earth observation satellite data. Glass, Vol. 102, pp. 101–102.

UNEP. (2007). Mangroves of Western and Central Africa. Retrieved from http://www.unep-wcmc.org/resources/publications/UNEP_WCMC_bio_series/26.htm

Wang, D., Wan, B., Qiu, P., Su, Y., Guo, Q., Wang, R., … Wu, X. (2018). Evaluating the performance of Sentinel-2, Landsat 8 and Pléiades-1 in mapping mangrove extent and species. Remote Sensing, 10(9). https://doi.org/10.3390/rs10091468

Wang, J., Rich, P. M., Price, K. P., & Dean Kettle, W. (2005). Relations between NDVI, grassland production, and crop yield in the central great plains. Geocarto International, 20(3), 5–11. https://doi.org/10.1080/10106040508542350

Wang, L., Sousa, W. P., & Gong, P. (2004). Integration of object-based and pixel-based classification for mapping mangroves with IKONOS imagery. International Journal of Remote Sensing, 25(24), 5655–5668. https://doi.org/10.1080/01431160233129121 5

Wang, Le, Jia, M., Yin, D., & Tian, J. (2019). A review of remote sensing for mangrove forests: 1956–2018. Remote Sensing of Environment, 231(June). https://doi.org/10.1016/j.rse.2019.111223

Wang, Le, Sousa, W. P., Gong, P., & Biging, G. S. (2004). Comparison of IKONOS and QuickBird images for mapping mangrove species on the Caribbean coast of Panama. Remote Sensing of Environment, 91(3–4), 432–440. https://doi.org/10.1016/j.rse.2004.04.005

Xie, Y., Sha, Z., & Yu, M. (2008). Remote sensing imagery in vegetation mapping: a review. Journal of Plant Ecology, 1(1), 9–23. https://doi.org/10.1093/jpe/rtm005

Yidana, S.M.; Banoeng-yakubo, B.; Akabzaa, T.M. (2010). Analysis of Groundwater Quality Using Multivariate and Spatial Analyses in the Keta Basin, Ghana. J. Afr. Earth Sci., 58, 220–234.

Younes Cárdenas, N., Joyce, K. E., & Maier, S. W. (2017). Monitoring mangrove forests: Are we taking full advantage of technology? International Journal of Applied Earth Observation and Geoinformation, 63(July), 1–14. https://doi.org/10.1016/j.jag.2017.07.004

Zulfa, A. W., & Norizah, K. (2018). Remotely sensed imagery data application in mangrove forest: A review. Pertanika Journal of Science and Technology, 26(3), 899–922.

APPENDIX

Python script for calculating mangrove area coverage from NDVI and CMRI maps

```
from osgeo import gdal

pix_min = 0.6
pix_max = 0.8
pixel_size = 10*10

path = r"D:\MASC_01\Thesis\Results\New folder\Final\NDVI_NEW.tif"
super_img = gdal.Open(path).ReadAsArray()
area = 0
others = 0
null_data=super_img[0][0]
for row in super_img:
    for cell in row:
        if (cell > pix_min) and (cell < pix_max):
            area += pixel_size
        elif cell != null_data:
            others += pixel_size

print (area)
print ((area*100)/(area+others))
print (area+others)
```